

Norrisanima miocaena, a new generic name and redescription of a stem balaenopteroid mysticete (Mammalia, Cetacea) from the Miocene of California (#29605)

1

First submission

Editor guidance

Please submit by **7 Feb 2019** for the benefit of the authors (and your \$200 publishing discount).



Structure and Criteria

Please read the 'Structure and Criteria' page for general guidance.



Custom checks

Make sure you include the custom checks shown below, in your review.



Author notes

Have you read the author notes on the [guidance page](#)?



Raw data check

Review the raw data. Download from the location [described by the author](#).



Image check

Check that figures and images have not been inappropriately manipulated.

Privacy reminder: If uploading an annotated PDF, remove identifiable information to remain anonymous.

Files

Download and review all files from the [materials page](#).

7 Figure file(s)

1 Table file(s)

1 Other file(s)



Custom checks

New species checks



Have you checked our [new species policies](#)?



Do you agree that it is a new species?




Is it correctly described e.g. meets ICZN standard?



Structure your review

The review form is divided into 5 sections. Please consider these when composing your review:

1. BASIC REPORTING
2. EXPERIMENTAL DESIGN
3. VALIDITY OF THE FINDINGS
4. General comments
5. Confidential notes to the editor






 You can also annotate this PDF and upload it as part of your review

When ready [submit online](#).





Editorial Criteria

Use these criteria points to structure your review. The full detailed editorial criteria is on your [guidance page](#).





BASIC REPORTING

-  Clear, unambiguous, professional English language used throughout.
-  Intro & background to show context. Literature well referenced & relevant.
-  Structure conforms to [PeerJ standards](#), discipline norm, or improved for clarity.
-  Figures are relevant, high quality, well labelled & described.
-  Raw data supplied (see [PeerJ policy](#)).

EXPERIMENTAL DESIGN

-  Original primary research within [Scope of the journal](#).
-  Research question well defined, relevant & meaningful. It is stated how the research fills an identified knowledge gap.
-  Rigorous investigation performed to a high technical & ethical standard.
-  Methods described with sufficient detail & information to replicate.

VALIDITY OF THE FINDINGS

-  Impact and novelty not assessed. Negative/inconclusive results accepted. *Meaningful* replication encouraged where rationale & benefit to literature is clearly stated.
-  Data is robust, statistically sound, & controlled.
-  Speculation is welcome, but should be identified as such.
-  Conclusions are well stated, linked to original research question & limited to supporting results.

Standout reviewing tips

3



The best reviewers use these techniques

Tip

Support criticisms with evidence from the text or from other sources

Example

Smith et al (J of Methodology, 2005, V3, pp 123) have shown that the analysis you use in Lines 241-250 is not the most appropriate for this situation. Please explain why you used this method.

Give specific suggestions on how to improve the manuscript

Your introduction needs more detail. I suggest that you improve the description at lines 57- 86 to provide more justification for your study (specifically, you should expand upon the knowledge gap being filled).

Comment on language and grammar issues

The English language should be improved to ensure that an international audience can clearly understand your text. Some examples where the language could be improved include lines 23, 77, 121, 128 – the current phrasing makes comprehension difficult.

Organize by importance of the issues, and number your points

1. Your most important issue
2. The next most important item
3. ...
4. The least important points

Please provide constructive criticism, and avoid personal opinions

I thank you for providing the raw data, however your supplemental files need more descriptive metadata identifiers to be useful to future readers. Although your results are compelling, the data analysis should be improved in the following ways: AA, BB, CC

Comment on strengths (as well as weaknesses) of the manuscript

I commend the authors for their extensive data set, compiled over many years of detailed fieldwork. In addition, the manuscript is clearly written in professional, unambiguous language. If there is a weakness, it is in the statistical analysis (as I have noted above) which should be improved upon before Acceptance.

***Norrisanima miocaena*, a new generic name and redescription of a stem balaenopteroid mysticete (Mammalia, Cetacea) from the Miocene of California**

Matthew S Leslie ^{Corresp., 1, 2}, **Carlos M. Peredo** ^{1, 3}, **Nicholas D Pyenson** ^{1, 4}

¹ Department of Paleobiology and Vertebrate Zoology, National Museum of Natural History, Smithsonian Institution, Washington, DC, United States

² Center for Conservation Genomics, Smithsonian Conservation Biology Institute, Washington, DC, United States

³ Environmental Science and Policy, George Mason University, Fairfax, VA, United States

⁴ Department of Paleontology and Geology, Burke Museum of Natural History and Culture, Seattle, Washington, United States

Corresponding Author: Matthew S Leslie

Email address: mleslie2@swartmore.edu

Large baleen whales (Mysticeti) known as rorquals are among the largest vertebrates ever, yet the monophyly of their traditional grouping (i.e., Balaenopteridae) remains unclear, especially regarding the position of gray whales (*Eschrichtius robustus* (Lilljeborg, 1861)), as either sister to a monophyletic Balaenopteridae or nested within a paraphyletic Balaenopteridae. Regardless of topology, gray whales and other rorquals together form the larger clade Balaenopteroidea, to the exclusion of all other mysticetes. Many fossil mysticetes putatively assigned to either Balaenopteridae or Balaenopteroidea may actually belong to stem lineages outside these crown groups, although many of these fossil taxa suffer from inadequate descriptions of fragmentary skeletal material. Here, we provide a new generic name and redescription for a stem balaenopteroid from the Monterey Formation of California, *Norrisanima miocaena*, gen. nov. Originally described as *Megaptera miocaena* in 1922, the holotype specimen includes a partial cranium, a fragment of the rostrum, a single vertebra, and tympanoperiotic material. Kellogg (1922) assigned the holotype specimen to the genus *Megaptera*, on the basis of its broad similarities to distinctive traits in the cranium of extant humpback whales (*Megaptera novaeangliae* (Borowski, 1781)). Subsequent phylogenetic analyses have found these two species as sister taxa in morphological datasets alone; the most recent systematic analyses using both molecular and morphological data sets place *Norrisanima miocaena* as a stem balaenopteroid unrelated to humpback whales. With this stem placement and an updated age estimate from associated microfossils (Tortonian, 7.6-7.3 Ma), we propose *N. miocaena* as a candidate fossil calibration point for dating the divergence of crown Balaenopteroidea, which potentially constrains the timing of the origin of important evolutionary innovations in this group, including gigantism and lunge-feeding.

Norrisanima miocaena, a new generic name and redescription of
a stem balaenopteroid mysticete (Mammalia, Cetacea) from the
Miocene of California

Matthew S. Leslie^{1,2*}, Carlos Mauricio Peredo^{1,3}, and Nicholas D. Pyenson^{1,4}

1. Department of Paleobiology and Vertebrate Zoology, National Museum of Natural History,
Smithsonian Institution, Washington DC, USA

2. Center for Conservation Genomics, Smithsonian Conservation Biology Institute, Smithsonian
Institution, Washington DC, USA

3. Department of Environmental Science and Policy, George Mason University, Fairfax, VA,
USA

4. Department of Paleontology and Geology, Burke Museum of Natural History and Culture,
1413 NE 45th Street, Seattle, WA 98105, USA

*Corresponding Author:

Matthew S. Leslie

Swarthmore College

500 College Ave, Swarthmore, PA 19081, USA

Email Address: matt.s.leslie@gmail.com

27 ABSTRACT

28 Large baleen whales (Mysticeti) known as rorquals are among the largest vertebrates ever, yet
 29 the monophyly of their traditional grouping (i.e., Balaenopteridae) remains unclear, especially
 30 regarding the position of gray whales (*Eschrichtius robustus* (Lilljeborg, 1861)), as either sister
 31 to a monophyletic Balaenopteridae or nested within a paraphyletic Balaenopteridae. Regardless
 32 of topology, gray whales and other rorquals together form the larger clade Balaenopteroidea, to
 33 the exclusion of all other mysticetes. Many fossil mysticetes putatively assigned to either
 34 Balaenopteridae or Balaenopteroidea may actually belong to stem lineages outside these crown
 35 groups, although many of these fossil taxa suffer from inadequate descriptions of fragmentary
 36 skeletal material. Here, we provide a new generic name and redescription for a stem
 37 balaenopteroid from the Monterey Formation of California, *Norrisanima miocaena*, gen. nov.
 38 Originally described as *Megaptera miocaena* in 1922, the holotype specimen includes a partial
 39 cranium, a fragment of the rostrum, a single vertebra, and tympanoperiotic material. Kellogg
 40 (1922) assigned the holotype specimen to the genus *Megaptera*, on the basis of its broad
 41 similarities to distinctive traits in the cranium of extant humpback whales (*Megaptera*
 42 *novaeangliae* (Borowski, 1781)). Subsequent phylogenetic analyses have found these two
 43 species as sister taxa in morphological datasets alone; the most recent systematic analyses using
 44 both molecular and morphological data sets place *Norrisanima miocaena* as a stem
 45 balaenopteroid unrelated to humpback whales. With this stem placement and an updated age
 46 estimate from associated microfossils (Tortonian, 7.6-7.3 Ma), we propose *N. miocaena* as a
 47 candidate fossil calibration point for dating the divergence of crown Balaenopteroidea, which
 48 potentially constrains the timing of the origin of important evolutionary innovations in this
 49 group, including gigantism and lunge-feeding.

Introduction

Rorqual whales include the largest vertebrates to have ever evolved in the history of life. Despite recent insights into evolutionary trends in body size for these taxa (Slater et al. 2017), the overall phylogenetic relationships among extant lineages of rorquals remain a work in progress (Árnason et al. 2018). Specifically, questions remain regarding the monophyly of Balaenopteridae (relative to *Eschrichtius robustus* (Lilleborg 1861)), or living gray whales) and the monophyly of the clade *Balaenoptera* Lacépède 1804 (with regard to the living genus *Megaptera* Gray 1846). Three main hypotheses for their relationships reoccur predominantly in the recent literature (e.g., Deméré et al. 2008; McGowen et al. 2009; Gatesy et al. 2013; Marx & Fordyce 2015; Marx & Kohno 2016; Slater et al. 2017; Árnason et al. 2018). The first is the traditional view of a monophyletic Eschrichtiidae and Balaenopteridae as sister clades with *Megaptera* sister to *Balaenoptera* within Balaenopteridae (Fig. 1A). This view matches classification schemes built in the 20th century (e.g., Rice 1998, and references therein) and the phylogenetic relationships derived from only morphological data sets (Marx 2011; Bosselaers & Post 2010; Boessenecker & Fordyce 2015), with the exception of a combined morphological and genetic data set (Geisler et al. 2017). The second reoccurring hypothesis (Fig. 1B) includes Eschrichtiidae nested within Balaenopteridae, and *Megaptera* within *Balaenoptera*. This overall pattern has been supported by molecular (McGowen et al. 2009; Sasaki et al. 2006) and combined morphological and molecular data sets (Marx & Fordyce 2015; Slater et al. 2017), including both fossil and extant taxa, as well from putative extinct members of Balaenopteridae and Eschrichtiidae *sensu lato* (Marx & Kohno 2016, Slater et al. 2017). By contrast, two molecular studies (McGowen et al. 2009; Sasaki et al. 2006) used only extant lineages, highlighting the inconsistent taxon sampling

across these studies. The third hypothesis (Fig. 1C) built from combined morphological and molecular data, or strictly molecular data, place Eschrichtiidae and Balaenopteridae as sister clades with *Megaptera* nested within *Balaenoptera* and sister to *B. physalus* (Linnaeus, 1758) (Sasaki et al. 2006, Deméré et al. 2008, Gatesy et al. 2013). This hypothesis also recovers a monophyletic Balaenopteridae but does not recover a monophyletic genus *Balaenoptera* (Fig 1C).

Norrisanima miocaena gen. nov. from the Monterey Formation of California is a stem balaenopteroid described nearly a century ago (Kellogg, 1922). Kellogg (1922) originally placed this species within the genus *Megaptera* based on the wide breadth of the cranium relative to its length and similarities in the tympanoperiotics. Deméré et al. (2005) noted, however, that *N. miocaena* lacks any of the autapomorphies of the extant *M. novaeangliae* (Borowski, 1781). Recent phylogenetic analyses based on morphological and molecular data sets have also failed to recover this putative congeneric sister relationship (Deméré et al. 2008; Gatesy et al. 2013; McGowen et al. 2009; Marx & Fordyce 2015; Marx & Kohno 2016; Slater et al. 2017). However, several exclusively morphological phylogenetic analyses have recovered *N. miocaena* in a sister relationship with extant *M. novaeangliae* (Marx 2011; Boessenecker & Fordyce 2015; Boessenecker & Fordyce 2017). Here we provide a morphological basis for discriminating the putative similarities that *N. miocaena* shares with *M. novaeangliae*, and highlight the balaenopteroid synapomorphies that it lacks, affirming its status as a stem balaenopteroid. These morphological observations supplement the existing phylogenetic framework, using comprehensive molecular and morphological datasets, which place *N. miocaena* outside of crown Balaenopteroidea (Marx & Kohno 2016; Slater et al. 2017). We thus follow Deméré et al.

(2005)'s recommendation and assign Kellogg (1922)'s specimen to a new generic name, *Norrisanima*.

N. miocaena provides several important lines of evidence for the evolution of rorqual whales. Although it is only mid-range in size compared to extant balaenopteroids, its estimated total length at 12.49 m (using Pyenson & Sponberg (2011)'s reconstruction equation for stem balaenopteroids) is among the larger stem balaenopteroids of its age (see late Miocene taxa in Figure 2 of Slater et al. 2017). Although it lacks a mandible, the glenoid fossa of the type specimen is broadly similar to extant rorquals, suggesting some basis for inferring lunge-feeding features in this taxon, although there are important soft tissue features that lack osteological correlates to strengthen this argument. Lastly, *N. miocaena* meets the criteria for a fossil calibration point (*fide* Parham et al. 2014) for phylogenetic divergence dating of crown Balaenopteroidea.

Methods

Anatomical terminology follows Mead & Fordyce (2009). Permits for collection were not required, as the specimen was collected near Lompoc, California in 1919 and has been accessioned at the Smithsonian Institution ever since. The updated age was determined by analysis of microfossils from matrix surrounding the cranium (see Akiba 1986).

Institutional Abbreviation

USNM, Departments of Paleobiology and Vertebrate Zoology (Division of Mammals), National Museum of Natural History, Smithsonian Institution, Washington, District of Columbia, USA.

3D surface scanning – cranium

We used an Artec Eva (Artec Europe, Luxembourg) hand-held structured light scanner to create a 3D model of the cranium of the holotype specimen (USNM 10300). Because of the size and weight of the type and only specimen, we scanned the dorsal and ventral sides separately. We scanned at a rate of two frames per second and completed several scans to cover the surface of each side. All data cleaning, processing, and model creation were completed in the Artec Studio12 software package. We imported all scans for the dorsal side into a single project and performed a global registration, then aligned each scan incrementally using a set of three shared landmarks in the Align Tool Function and finished by cleaning and trimming the scan to remove data collected from the specimen housing jacket. The process was then repeated for the ventral side. Thus, scans from each side were aligned and trimmed in isolation from the other to create a composite model for each side. Then, we conducted a final global registration on the two models and again used the Align Tool to join the two halves into a single, final 3D model. We then completed another global registration and created a complete 3D model using the Fast Fusion tool; this model was not watertight. Holes in the model up to and including 150 pixels were filled using the Hole Fill tool; all other holes were left open. Most of the holes occurred in deep recesses where the scanner could not collect data, or where the storage jacket obscured both the dorsal and ventral sides of the cranium. Once the model was complete, we exported it as STL format for the distributed model (available in Supplemental Material), and for import into MeshLab (Cignoni et al. 2008) where we exported PNG image files.

CT scanning – tympanoperiotics

We scanned **three of the four tympanoperiotics** from the holotype at the Smithsonian Institution Bio-Imaging Research Center in the Department of Anthropology at the National Museum of Natural History in Washington, D.C., U.S.A. Computed tomography (CT) data were collected with a Siemens Somatom Emotion 6 (Siemens Medical Solutions, Erlangen, Germany) at slice thickness of 0.63 mm, resulting in a 3D reconstruction increment of 0.30 mm. DICOM files were processed by importing image files in Mimics Innovation Suite 19 (Materialise NV, Leuven, Belgium). In Mimics, we created a mask based on the threshold of bone relative to the nominal density of air. A 3D object was then created from this mask, and exported as a binary STL file. The STL file was then opened in MeshLab (Cignoni et al. 2008) for final editing to create 3D models and figures of the external morphology.

Phylogenetic nomenclature

We followed the recommendations of Joyce, Parham & Gauthier (2004) for the conversion of select ranked taxonomic cetacean names to phylogenetically defined ones in this study, following similar steps by Pyenson et al. (2015). For these purposes, we used abbreviations NCN for New Clade Name and CCN for Converted Clade Name. Below, we clarify our precise definitions for these clades (see PhyloCode, 2014, Article 9.3; Cantino & de Queiroz, 2014), and we also provide full citations for the names of specifier species.

Nomenclatural acts

The electronic version of this article adheres to the amended International Code of Zoological Nomenclature (ICZN). Specifically, the new name contained in this work is available under the ICZN from the electronic version of this article. Both the nomenclatural acts and the published

work itself are registered in ZooBank, the online registration system for the ICZN. The ZooBank Life Science Identifiers and the associated information can be viewed online by appending the LSID to the prefix “http://zoobank.org/” in any web-browser. The LSID for this publication is: [urn:lsid:zoobank.org:act:E777170E-03BC-40AA-A04B-65CE92C956BD](http://zoobank.org/urn:lsid:zoobank.org:act:E777170E-03BC-40AA-A04B-65CE92C956BD)

Results

1. Systematic paleontology

MAMMALIA Linneaus, 1758

CETACEA Brisson, 1762

PELAGICETI Uhen, 2008

NEOCETI Fordyce & de Muizon, 2001

MYSTICETI Gray, 1864

PLICOGULAE Geisler et al. 2011

PAN BALAENOPTEROIDEA (NCN) (panstem-based version of Balaenopteroidea Gray 1868)

Norrisanima ~~miocaena~~, nov. gen., [urn:lsid:zoobank.org:act:E777170E-03BC-40AA-A04B-65CE92C956BD](http://zoobank.org/urn:lsid:zoobank.org:act:E777170E-03BC-40AA-A04B-65CE92C956BD)

Definitions: ‘Pan-Balaenopteroidea’ refers to the panstem that includes crown Balaenopteroidea (CCN), and all other lineages closer to *Balaenoptera* Lacépède, 1804 than to *Caperea* Gray, 1864, such as *Pelocetus calvertensis* Kellogg, 1965, *Norrisanima miocaena* and *Parabalaenoptera bauliensis* Zeigler et al. 1997. Crown group Balaenopteroidea refers to the crown clade arising from the last common ancestor of *Eschrichtius* and all named

extant species of *Balaenoptera*. Given the potential paraphyly of the family Balaenopteridae and the genus *Balaenoptera* (see Introduction), we elect not to formalize crown concepts for these taxonomic group at this time.

Type and only known species: *Norrisanima*, ~~nov. gen.~~, *miocaena*.

Etymology: Combining the surname Norris and the Latin *anima* (breath of life), the generic name honors Norris *pere et fils*, the late Dr. Kenneth S. Norris and his son, Dr. Richard D. Norris, for their contributions to the natural history of California, marine mammalogy, and evolution in the marine realm. K. S. Norris was a founder of the Society for Marine Mammalogy and its first president, as well the founder of the University of California Natural Reserve System. Aside from the holotype specimen's provenance from southern California, the epithet also honors the teaching and mentorship legacies of both Norrises at various campuses of the University of California, including the Scripps Institution of Oceanography, where R. D. Norris served on MSL's doctoral dissertation committee.

Diagnosis: Same as that of the only known species *Norrisanima miocaena*, new combination Figs 2-5.

Holotype: Same as that of the only known species.

Type Locality: Same as that of the only known species.

209 **Formation:** Same as that of the only known species.

210

211 **Age:** Same as that of the only known species.

212 *Norrisanima miocaena*, new combination, [urn:lsid:zoobank.org:act:E777170E-03BC-40AA-](https://zoobank.org/urn:lsid:zoobank.org:act:E777170E-03BC-40AA-A04B-65CE92C956BD)

213 [A04B-65CE92C956BD](https://zoobank.org/urn:lsid:zoobank.org:act:E777170E-03BC-40AA-A04B-65CE92C956BD)

214

215 **Diagnosis:** *N. miocaena* is a stem balaenopteroid that possesses the following autapomorphies:

216 the lateral margins of the nasal are parallel, spreading of the anterolateral portion of the parietal

217 on to the posteromedial corner of the supraorbital process of the frontal; the anteriormost point of

218 the supraoccipital in dorsal view is in line with the anterior half or anterior edge of the

219 supraorbital process; the zygomatic process of the squamosal is distinctly higher dorsoventrally

220 than wide transversely, having a squared anterior apex of the supraoccipital shield, showing a

221 rounded outline of the supraoccipital in dorsal view; the tip of the postglenoid process pointing

222 ventrally in lateral view, lacking a distinct ridge delimiting the insertion surface of tensor

223 tympani on medial side of the anterior process of the periotic; and having a superior process of

224 the periotic present as a distinct crest forming the lateral wall of the suprameatal fossa.

225

226 **Holotype:** USNM 10300 is an incomplete cranium, including both tympanoperiotics as isolated

227 material, an isolated vertebra, and a disarticulated piece of the rostrum. Kellogg (1922) reported

228 that the anterior portion of the rostrum and much of the right side of the skull were damaged or

229 destroyed during excavation. In addition, the palatines were damaged during transport to the

230 Smithsonian Institution. Additional plaster has been added since the original description—

231 particularly to hold parts of the right side of the cranium (squamosal, zygomatic arch, and

maxilla) together. The disarticulated rostral piece is most likely from the left maxilla, though there are no patent connections. The right tympanic was also damaged, but most of the fragments were recovered and reconstructed. The right periotic is missing its posterior process but is otherwise complete.

Type Locality: The main Celite quarry of the Lompoc diatomite mines (after the Celite Corporation), also called the Johns-Manville quarry (after the Johns-Manville Company), near Lompoc, California, U.S.A. Kellogg (1922) described the type locality as “one-half mile northwest of the northeast corner of township 6 north, range 34 west (Lompoc Quadrangle), on top of divide between drainage of San Miguelito Creek and Salsipuedes Creek, 3 miles south and east of Lompoc, Santa Barbara County, California.” Using Google Earth and the current Lompoc Hills Quadrangle map (USGS NGA Ref No: X24K26325), which includes the township 6 borders, the approximate GPS coordinates for the excavation site are 34° 36’ 56” N; 120° 26’ 43” W with a margin of error of approximately 0.5 miles. The Celite quarry is equivalent to the Johns-Manville quarry (see Dibblee, 1950), but separate from the nearby Great Lakes Carbon Corporation quarry (which is the type locality of the fossil odobenid *Imagotaria downsi* Mitchell, 1968) and very likely separate from Celite Quarry No. 9, which is the type locality of the fossil crown otariid *Pithanotaria starri* Kellogg, 1925, and also separate from the main Celite quarry; see Repenning and Tedford (1977).

Formation: Monterey Formation.

Age: Late Tortonian, between 7.6–7.3 Ma. Kellogg (1922) reported that the type specimen was discovered by quarrymen at the Celite Products Company (now Celite Corporation, or generally Celite) diatomite mines in Lompoc, California, in a horizon “about 150 feet below the quarry’s surface” at the type locality. Kellogg (1922) noted, at the time, that a precise determination of the type specimen’s stratigraphic origin would not be possible until the quarry deepened to that latter depth; to our knowledge, this determination never happened. At the time of Kellogg (1922)’s description, Kellogg correlated the Lompoc diatomite mines with the Temblor Formation (roughly middle to late Miocene), while work throughout the 20th century eventually assigned the Lompoc diatomites to the Monterey Formation. Relying on work by Kleinpell (1938) and Barron (1986), Behl et al. (2000) reported a late Miocene age for the Lompoc diatomites between 8.5–5.5 Ma (Tortonian to Messinian). Later, Barron and Isaacs (2001) revised the age of the Lompoc diatomites to 9.2–6.8 Ma, based on a detailed chronostratigraphic framework of the Monterey Formation. Deméré et al. (2005) argued that the Lompoc diatomites should be Tortonian in age (8.2–7.3 Ma), following Chang and Grimm (1999). Marx and Fordyce (2015) cited Chang and Grimm (1999)’s upper age boundary of 7.3 Ma on the 218 m sequence of mineable diatomite exposed at the Celite quarry (reported as J. A. Barron, pers. comm., 1997) along with unpublished data from N. Kohno (pers. comm., 2010), who assigned diatoms collected from the matrix surrounding the cranium of *N. miocaena* to the *Rouxia californica* diatom subzone (NPD7A) of Akiba (1986). The NPD7A subzone now ranges across the current boundaries of the Tortonian and Messinian with an age range of 7.6–6.5 Ma (see Barron et al. 2001), with the older age providing a lower age bound. Thus, Marx and Fordyce (2015) argued that the preponderance of evidence points to a 7.6–7.3 Ma age for the type specimen of *N. miocaena*.

277

278 **Comments:** Fossil material from the Funakawa Formation (upper Miocene) of Akita, Japan
 279 (Oishi and Hasegawa 1995) and isolated tympanic material from the Tatsunokuchi and Na-arai
 280 formations (Lower Pliocene) of northeastern Honshu, Japan have been tentatively assigned to
 281 this taxon (Deméré et al. 2005). The authors have not viewed this material and therefore cannot
 282 comment on its affinity.

283

284

285 **Description**

286

287 **Cranium (Figs. 2-3)**

288 **Premaxilla**

289 In dorsal view, the premaxilla is exposed along the mesorostral groove, then narrows posteriorly.
 290 The left premaxilla is fragmented into a sharp point anteriorly with a medial deflection so that its
 291 medial margin extends posterior to its lateral margin, terminating at about the level of the
 292 anterior margin of the nasal. The ascending process of the premaxilla is incomplete where it
 293 abuts the left nasal, leaving an open suture. We suspect that, in life, the ascending process of the
 294 maxilla likely would have abutted or overlapped the ascending process of the premaxilla near the
 295 nasal. Finally, the premaxilla is situated dorsally above the maxilla, so the rostrum slopes
 296 ventrally toward the lateral margin.

297

298 **Maxilla**

299 The right maxilla is damaged and almost entirely lost. The anterior section of the left maxilla is
 300 damaged and lost and the posterior portion of the ascending process of the left maxilla appears to
 301 be lost as well, revealing a slight depression lateral to the left nasal. In dorsal view, both the
 302 medial and lateral margins of the maxilla parallel the sagittal plane. The medial margin of the
 303 maxilla has a slight concavity, whereas the lateral margin is straight. Overall, the maxilla
 304 broadens posteriorly where it transitions to the rest of the cranium. In the posteromedial corner
 305 the maxilla broadens with a triangular ascending process, extending medially over the premaxilla
 306 and the parietal. The posterior margin of the maxilla abuts the frontal in a nearly transverse
 307 suture, which curves posterolaterally toward the orbit. At the lateral margin, the maxilla lies
 308 ventral to the frontal creating a shallow antorbital notch. In anterior view, the maxilla is elevated
 309 dorsally at the medially margin where it contacts the premaxilla and descends ventrally at the
 310 lateral margin. Two deep pits in the rostral portion of the maxilla may represent maxillary
 311 foramen.

312

313 In ventral view, the lateral margin of the maxilla is parallel with the sagittal plane until the level
 314 of the neurocranium where it deflects laterally. The medial margin is damaged, but can clearly be
 315 seen underlying the vomer. The posterior margin of the maxilla is also fragmented, making it
 316 difficult to discriminate an infraorbital plate laterally. Medially, the posterior margin underlies
 317 the palatine. The posteromedial corner of the maxilla is poorly preserved. Clear foramina and
 318 sulci are present along the whole ventral surface of the maxilla, likely representing the presence
 319 of the neurovasculature to support baleen in life. The foramina and sulci angle posterolaterally,
 320 and angle increasingly lateral moving anteriorly. A triangle-shaped trough lies at the
 321 posterolateral corner of the maxilla, anteroventral to the preorbital process of frontal (this feature

is visible in other extant balaenopterids). The two maxillae would likely have contacted each other at the midline (possibly with the anterior portion of the vomer visible near the mesorostral groove), but we cannot be certain because of the missing portion of the right maxilla.

Nasal

Overall the nasals are short and rectangular, being longer anteroposteriorly than transversely wide. In dorsal view, the left nasal is complete and in its original articulation, but the ascending process of the left premaxilla is missing, leaving a gap between ascending process of the maxilla and the left nasal. The posterior margin of the nasals abuts the anterior margin of the supraoccipital. The anterior margin curves anteriorly at the lateral corner. An anterolateral projection parallels the premaxilla and creates the posterolateral border of the mesorostral groove. Together, the anterior margins of both nasals overall slope anteroventrally, descending into the mesorostral groove.

Palatine

In ventral view, the anterior portion of the palatine is fragmented and it was difficult to determine a clear anterior suture with the maxilla. The lateral margin of the palatine wraps dorsally, and forms the medial margin of the frontal. Posteriorly the palatine fuses with the pterygoid, but the suture is damaged, so it is difficult to determine where the fusion occurs. The palatine slopes ventrally toward the midline where it underlies the vomerine crest.

Vomer

344 In ventral view, the vomerine crest appears below the palatine at the level of the distal opening of
 345 the orbital canal. It rises as it progresses posteriorly and extends under the basisphenoid to the
 346 level between the basioccipital crests. At its visible anterior end in the basicranium, the vomer is
 347 transversely swollen and narrows posteriorly to form a rounded ridge. The surfaces of the vomer
 348 that line the internal choanae are damaged anteriorly, but the shape is clear, with anterior
 349 portions that are wide relative to the posterior end, and terminate near the pterygoid-basioccipital
 350 suture, anteromedial to the bulbous portion of the basioccipital crests. The lateral and medial
 351 margins are ventrally deflected to create a deep dorsal arch between each basioccipital crest and
 352 the vomerine crest. Posteriorly, the nasal plate of the vomer extends underlies the basioccipital.
 353

354 Frontal

355 In dorsal view, the frontal is broadly rectangular with the lateral and medial margins shorter than
 356 the anterior and posterior margins. The frontal is long anteroposteriorly and its anterior margin
 357 abuts the maxilla at a suture that is nearly transverse in orientation. In a lateral view of the
 358 supraorbital process of the frontal, there is a shallow depression at this anterior suture that
 359 Deméré et al. (2005) termed an “incipient balaenopterid ‘pocket,’” although this structure in
 360 other rorquals is largely a construction of more of the maxilla than the frontal, and the poor
 361 preservation of the type of *N. miocaena* precludes speculation about its original morphology. In
 362 oblique dorsolateral view, the medial margin of the front seems to contact the parietal just before
 363 the parietal rises to the vertex, excluding the frontal’s participation in the vertex.

364

365 The preorbital process of the frontal is directly posterior to the lateral termination of the
 366 antorbital notch of the maxilla. The postorbital process extends slightly further laterally in

relation to the preorbital process. The medial margin of the frontal near the temporal wall is dorsally elevated so the lateral margin slopes ventrally. Posteriorly, the frontal is robust and dorsoventrally thickened where it makes up the margin of the temporal fossa. Beginning with the contact of the postorbital process and the zygomatic process of the squamosal, a blunt ridge extends anteromedially to about the level of the midpoint of the orbit. This ridge likely demarcates a lateral margin of the temporalis.

In ventral view, the anterior margin of the frontal appears to have a transverse suture with the maxilla overriding it, although poor preservation makes it difficult to ascertain the extent of infraorbital plate of the maxilla overlying it. Medially, the ventral surface of the frontal borders the palatine. The optic canal is deeply concave with posterior and anterior margins (medially) that are dramatically curved ventrally and almost touching. Moving laterally along the optic canal, the frontal expands anteroposteriorly into the orbit. The preorbital process points anteroventrally, but does not underlie the maxilla. The postorbital process contacts the zygomatic process of the squamosal. No jugal or lacrimal are preserved.

Parietal

In dorsal view, near the vertex, the parietal is minimally exposed as a small triangle between the frontal, supraoccipital, and the ascending process of the maxilla. Exposure broadens laterally, so the parietal is exposed at some length below the overhanging nuchal crest and dorsomedial to the frontal. The presence of an interparietal cannot be determined.

The surface of the parietal in the temporal wall is somewhat damaged. Posteriorly, the parietal is a vertical wall descending from the nuchal crest to the frontal, and joining it at nearly 90° angle. In lateral view the wall narrows posteriorly. The nuchal crest overhangs the vertical part of the parietal substantially. Posteriorly, the parietal pinches as it passes the posterior extent of the frontal then dorsoventrally expands greatly in the temporal wall where it forms a sigmoidal suture with the squamosal, at the posterior margin of the temporal fossa. This sigmoidal shaped contact between the parietal and the squamosal is not illustrated because of the limitations in 3D model reconstruction that prevent a lateral illustration of the type material.

Supraoccipital

The sutures between the supraoccipital, exoccipital, and basioccipital are tightly ankylosed. In dorsal view, the general shape of the supraoccipital is neither triangular nor circular, but trapezoidal with a squared-off anterior margin. The lateral margins broaden posteriorly. The supraoccipital shield is deflected forward so it overlies the frontal and parietals and abuts the nasals anteriorly at the vertex. It is relatively flat with no sagittal crest or obvious foramina or sulci. The nuchal crest comprises the lateral border of the supraoccipital at the supraoccipital-squamosal suture where it rises anteromedially as the continuation of the mastoid crest of the squamosal. Dorsal condyloid foramina are present on both sides.

Exoccipital

In ventral view, there is a gentle posterolateral deflection of the exoccipital. In lateral view, the paroccipital process is dorsoventrally aligned and flat (i.e., not tilted) and thickened anteroposteriorly. The posterior surface of the paraoccipital is posteriorly equal to the level of the

occipital condyles. In posterior view, the occipital condyles are reniform in shape and transversely broader ventrally than dorsally. They are large relative to the basioccipital crests and lie nearly in a dorsoventral plane. The occipital condyles are dorsoventrally oriented with lateral margins strongly convex and medial margins straight. There is a narrow ventral intercondylar notch and a broad dorsal intercondylar notch. In dorsal view, the occipital condyles are squat against the exoccipital.

418

419 **Basioccipital**

In ventral view, the anterior margin of the basioccipital is obscured by the nasal plates of the vomer. The lateral margin of the basioccipital is the pterygoid sinus fossa. The basioccipital is flat between the basioccipital crests. The crests are massive and rounded (i.e., bulbous). The bone overlying the jugular notch, which deflected laterally at a 45° angle from the midline, is robust and nearly forms an arch.

425

426 **Squamosal**

The squamosal is robust medially at the position of the mastoid crest where it abuts the supraoccipital and exoccipital, and pinches and slants anteroposteriorly as it extends anterolaterally becoming the zygomatic process. In dorsal view, the anterolateral margin of the squamosal angles slightly anteroventrally where it forms the posterior margin of the temporal fossa. Medially, this line moves into the temporal wall and borders the pterygoid to form the lateral border pterygoid sinus fossa.

433

In ventral view, the squamosal is large and robust with a deep glenoid fossa and large bulbous postglenoid process. The postglenoid process extends more ventrally than posteriorly, but has an anterior hook at the lateral margin that slightly encloses the glenoid fossa laterally and posteriorly. In lateral view, the anterior margin of the squamosal is very dorsoventral oriented, instead of anteroposterior. Medially the squamosal ascends dorsally from below the nuchal crest where it abuts the parietal. The postglenoid process is the most ventral portion of the cranium far below the plane of the basioccipital crests. In posterior view, the nuchal crest becomes the mastoid crest at about the level of the dorsal termination of the occipital condyles.

The zygomatic process is anteroposteriorly short but dorsoventrally robust and contacts the postorbital process of the frontal. It appears short because it directly abuts the postorbital process of the frontal. Its overall axis has an anterolateral deflection and is not straight anteroposteriorly. The ventral anterior portion of the right zygomatic process is damaged, but is not missing. The zygomatic process is taller dorsoventrally than it is transversely wide or anteroposteriorly long.

Pterygoid

In ventral view, the pterygoid sinus is a large and deep renal-shaped cavity that tapers slightly posteriorly. The roof of pterygoid sinus is overlain and enclosed posterodorsally by the squamosal. The medial surface the pterygoid forms the lateral surface of the internal nares, before undercutting to floor the nares; the pterygoid hamulus is broken. The lateral surface of the pterygoid rises from the pterygoid fossa up into the temporal wall.

Tympanic Bulla (Fig. 4)

In dorsal view, the tympanic bulla is overall square shaped. It has a sigmoid-shaped medial margin resulting from a shallow medial furrow. The posterior edge has rounded prominences (the medial prominence is transversely broader) separated by a shallow interprominental notch. The medial posterior prominence has a rounded transition to the medial margin of the bulla, whereas the lateral posterior prominence transitions to the lateral margin at a sharp angle. The anterior margin is broadly transverse but rounded on each edge and slightly slanted anteriorly toward the lateral margin. The lateral surface is broadly convex anteriorly, before transitioning to a pronounced lateral deflection at the level of the sigmoid process. As a result, a deep lateral furrow separates the middle portion from the anterior portion. Continuing posteriorly from the sigmoid process the lateral margin is straight in the sagittal plane.

The eustachian notch is broad and strongly deflected medially. The anterior portion of the outer lip is broken so the anterior pedicle is not present. The sigmoid process is poorly preserved and separate from the body of the bulla, but a contact can be inferred. It originates from the level of the lateral furrow and overlays the tympanic cavity with a posterior deflection. The posterior pedicle is not preserved. The involucrum is transversely broad posteriorly and narrows anteriorly. Posteriorly it is smooth, but there are anterior transverse sulci emanating from the eustachian notch.

In ventral view, its surface is smooth throughout the body of the bulla, except the medial margin where rugose pitting is visible. Although there is some damage to the outer lip, the anterolateral corner is inflated and globular, creating a distinct lobe bound posteriorly by the lateral furrow. There is no anterolateral shelf.

480

481 In lateral view, the bulla is somewhat ovoid. The anterior margin is dorsoventrally aligned and
482 transitions gently into the smooth convex ventral margin. The ventral margin ends abruptly at the
483 lateral posterior prominence and angles sharply anteriorly as it becomes the posterior margin.
484 This serves to pinch of the lateral posterior prominence and culminates in a rounded anterodorsal
485 ridge. The lateral furrow is mostly dorsoventral with a very slight posterior slant dorsally. It is
486 deep and broad anteroposteriorly at the ventrally edge and narrows dorsally. In lateral view the
487 posterior deflection of the sigmoid process is readily apparent, such that it extends posterior to
488 the conical process. An elongate projection of the sigmoid process is preserved, but not modeled
489 because it is a separate fragment. Anterior to the sigmoid process, the conical process is
490 preserved as a blunted peak. Damage to the lateral surface prevents interpretation of the malleal
491 ridge and sigmoidal cleft.

492

493 In medial view, the involucrum is massively globular posteriorly and narrows anteriorly. The
494 involucral ridge is shallow, and oriented anteroposteriorly with a very slight ventral convexity.
495 This ridge is nearly parallel to the main ridge and separated from it by a band of rugose and
496 deeply pitted bone. The medial posterior prominence is bulbous and smooth with a
497 dorsoventrally straight posterior margin. The median furrow has a slight anterior slant.

498

499 **Periotic (Fig. 5)**

500 Of the two periotics preserved in the type specimen, the right periotic is better preserved and
501 provides of the basis for the following description. In dorsal view, the periotic is roughly L-
502 shaped, and consists of a triangular anterior process and two medial projections of the pars

503 cochlearis. The posterolateral angle of the periotic is the triangular flange of the **venterolateral**
504 **tuberosity**; the posterior process for both periotics **remains preserved in situ** with the skull. The
505 lateral border of the anterior process is rounded anteriorly and deflected medially, while the
506 medial edge is straight and dorsoventrally oriented. **The most lateral portion of the periotic is the**
507 **juncture between the pars cochlearis and the anterior process.** The posterior edge of the pars
508 cochlearis exhibits a shallow concavity, bordered laterally by the level of the caudal tympanic
509 process. The **external anterior margin** of the more anterior of the **two projection of the medial**
510 **extension of the pars cochlearis** is straight and posteromedially oriented. The internal margin of
511 this projection is rugose, but prominent. The more posterior of the two projections follows the
512 same aspect but is not as long in the medial direction.

513

514 **In ventral view, the lateral margin** of the anterior process of the periotic is smooth and curved
515 medially. The **anterolateral** sulcus is present **at** following an anteroposterior direction offset
516 laterally from the anterior tip of the anterior process. The medial margin of the anterior process is
517 sinusoidal and terminates posteriorly near the **hiatus fallopian**. **The hiatus fallopian** wraps
518 posterolaterally around the base of the smooth surface of the cochlea. The posteromedial
519 termination of the hiatus fallopian is ventral to, and **obscures the opening of the fenestra ovalis**
520 near the triangular flange of the ~~ventro~~lateral tuberosity. Adjacent and anterolaterally to the
521 termination of the hiatus fallopian is **malleolar fossa**. Also slightly obscured in ventral view, **at the**
522 **anterior portion of the fenestra ovalis** is a **prominent** stapes. The lateral margin of the cochlea is
523 relatively straight, but turns medially abruptly as it transitions into the posterior margin. Ventral
524 to the posterior margin of the cochlea is the fenestra rotunda.

525

526 In medial view, the periotic appears as two distinct sections, the anterior process (which is
 527 roughly conical in shape) and the posterior and much larger pars cochlearis (which appears
 528 roughly spheroid with a posterior projection off the ~~dorsoposterior~~ corner – the lateral ridges of
 529 the triangular flange of the ~~ventro~~lateral tuberosity. Ventral to and midway between the two
 530 projections of the anteromedially tapering of pars cochlearis is the internal auditory meatus.
 531 Many of the features of the internal auditory meatus and area surrounding, that are usually
 532 visible in ventral view, are shifted to the ventromedial surface; these features are best viewed in
 533 medial view. Ekdale et al. (2011) described ontogenetic changes in the shape and depth of the
 534 internal auditory meatus in *Megaptera novaeangliae*. The holotype periotic of *N. miocaena*
 535 demonstrates characteristics identified by these authors as indicative of an ontogenetically
 536 mature individual: 1) a nearly circular shared aperture for both the facial canal (CNVII), and 2)
 537 the vestibulocochlear aqueduct (CNVIII) separated by a deeply recessed crista transversa. The
 538 crista transversa runs relatively straight anteroposteriorly with the facial canal on the ventral side
 539 and the vestibulocochlear canal on the dorsal side. Posterior to the internal auditory meatus and
 540 slightly posterior, is the recessed and dorsoventrally elliptical opening of the paralympathic and
 541 endolymphatic foramina.

542

543 In lateral view, the periotic is flat along the dorsal margin aside from a concavity near the
 544 midline of the anterior process. The ventral margin of the anterior process is also relatively flat
 545 and terminates posteriorly at the cochlea. The cochlea protrudes ventrally quite abruptly before
 546 curving posteriorly and then sloping back toward the dorsoposterior corner. Before reaching the
 547 triangular flange of the ~~ventro~~lateral tuberosity, the posterior margin is interrupted by the

invagination of the fenestra ovalis that reaches up posteroventrally and houses the stapes near its termination.

Discussion

Norrisanima compared with crown balaenopteroids

In a recent phylogenetic analysis of mysticetes using morphological and molecular data, Slater et al. (2017) showed *Norrisanima* represented a lineage positioned well outside of the extant genus *Balaenoptera*, and not sister to *M. novaeangliae*, and only distantly related to *Eschrichtius*. The morphological partition of Slater et al. (2017)'s analysis (which was based on Marx & Fordyce, 2015) shows seven synapomorphies uniting *Balaenopteroidea*: 1) a straight posterior border of the supraorbital process in dorsal view; 2) a short postorbital process that does not markedly project in any direction; 3) an optic canal that in ventral view is enclosed medially by bony laminae; 4) a well-developed and thickened postorbital ridge along the medial portion of the optic canal; 5) flattened dorsal surface of the nasal bones; 6) inflated posterior corner of the pars cochlearis (medial to the fenestra rotunda) that extends posteriorly beyond the fenestra rotunda; and 7) absent or indistinct medial lobe of the tympanic bulla. *Norrisanima* exhibits only one of these seven synapomorphies: the flattened nasal bones. This trait is a marked departure from the rounded condition of some stem mysticetes, and some crown mysticetes (and even *Balaenoptera* spp.) exhibit nasals with a peak or crest extending to the midline. Although there is no right nasal in the holotype of *Norrisanima*, the left nasal is clearly flat and only curves ventrally at the anterior-most margin as it dives into the mesorostral groove.

The other six traits separate *Norrisanima* from crown Balaenopteroidea. Instead of a straight posterior edge of the supraorbital process, *Norrisanima* has a slightly concave margin. Like extant Balaenopteroidea, *Norrisanima* does have a short postorbital process, but it is deflected posteriorly instead of laterally as in extant balaenopteroids. The medial portion of the optic canal is open ventrally in *Norrisanima*, although anterior and posterior margins of the optic canal do extent ventrally toward the medial end of the canal, and are almost touching. This appears to be somewhat intermediate between stem and extant balaenopteroids, which have closed optical canals medially. *Norrisanima* clearly has a postorbital ridge, but it is not as thick as modern rorquals, nor does it displace the optical canal from the posterior border of the supraorbital process as in extant balaenopteroids.

Broadly, the entire vertex of *Norrisanima* is very reminiscent of extant balaenopteroids, especially large species in the genus *Balaenoptera*, such as *Balaenoptera musculus* Linnaeus, 1758 and *Balaenoptera physalus* (Fig. 6). In both of these latter species, the nasals and ascending processes of the premaxillae meet the anterior margin of the supraoccipital shield in a transverse line that is nearly rectilinear for all the element terminations involved (unlike, for example, the posterior pinching of the nasals in *B. acutorostrata* Lacépède, 1804. However, in *Norrisanima*, the position of this configuration of the vertex relative to the level of orbit is most similar to *B. acutorostrata*, nearly at the midway level between the pre- and postorbital processes of the frontal. The dorsal profiles of nasal in *Norrisanima*, in particular, shares broad rectangular features with *Eubalaena australis* (Desmoulins, 1822) and an anterolateral spur similar to those found in some *B. edeni* Anderson 1878 (Omura et al. 1981)

594 The tympanoperiotics of *Norrisanima* show two traits that are not shared with extant
 595 balaenopteroids, although the differences are subtle (Fig. 7). Extant balaenopteroids have an
 596 inflated and posteriorly projecting caudal tympanic process of the pars cochlearis ~~on their~~
 597 ~~periotics~~ (Ekdale et al. 2011) that extends posteriorly to beyond the level of the fenestra rotunda.
 598 *Norrisanima* has an enlarged, but rounded, posteromedial corner of the pars cochlearis that is in
 599 line with the fenestra rotunda. Extant balaenopteroids do not have medial lobes on their tympanic
 600 bullae, or these medial lobes are indistinct. *Norrisanima* has a medial lobe on the bulla that is
 601 equal in size to the lateral lobe.

602

603 Because of the taxonomic legacy of this specimen, we further compared *Norrisanima* with
 604 *Megaptera* and ~~other~~ *Balaenoptera* spp., focusing on the periotics, which possess a large number
 605 of diagnostic cetacean traits (Ekdale et al. 2011). This process was performed in two stages: first,
 606 we compared *Megaptera* and *Balaenoptera* to develop a list of traits in which the two generally
 607 differ; then we compared *Norrisanima* to each genus within the context of these traits. These
 608 traits are not meant to be diagnostic nor exhaustive, and are merely heuristic; *Norrisanima* is
 609 formally diagnosed above according to previous phylogenetic analyses, not using this set of
 610 traits.

611

612 We examined the following periotic specimens in the USNM collections of the Department of
 613 Vertebrate Zoology (all right periotics except where noted): *M. novaeangliae* (USNM 486175),
 614 *Balaenoptera borealis* Lesson, 1828 (USNM 504699), *B. physalus* (USNM 237566—left
 615 periotic), and *Balaenoptera bonaerensis* Burmeister, 1867 (USNM 504953) and found ten
 616 characters that broadly distinguish the two genera (listed in Table S1). *M. novaeangliae* periotics

broadly differ from other *Balaenoptera* periotics in ten features, including: (1) the apertures of the cranial nerve ducts erupt in a deep recess in the medial margin of the pars cochlearis; (2) the apertures of the cranial nerve ducts open medially, without a dorsal deflection found in *Balaenoptera*; (3) a dorsoventrally flattened and mediolaterally elongate pars cochlearis; (4) a short and robust anterior process relative to the size of the pars cochlearis; (5) a lateral crest on the ventral surface of the anterior process; (6) a sharply pointed triangular flange of the ~~ventero~~lateral tuberosity; (7) a posteriorly deflected triangular flange; (8) a concave medial margin of the pars cochlearis (in dorsal and ventral view); (9) a transverse ridge on the ventral surface of the pars cochlearis; and (10) a deep invagination of the fenestra ovalis that almost completely obscures the stapes.

Norrisanima shares six traits with *Megaptera* and four with *Balaenoptera* (Table 1). The six characters shared with *Megaptera* include: (1) the apertures of the cranial nerve ducts erupt in a deep recess in the medial margin of the pars cochlearis; (2) the apertures of the cranial nerve ducts open medial, without a dorsal deflection ~~found in *Balaenoptera*~~; (3) a dorsoventrally flattening and mediolaterally elongation of the pars cochlearis; (4) a short and robust anterior process relative to the size of the pars cochlearis; (5) a concave medial margin of the pars cochlearis (in dorsal and ventral view); and (6) a deep invagination of the fenestra ovalis that almost completely obscures the stapes. The four traits that *Norrisanima* shares with *Balaenoptera* include: (1) the lack of a lateral crest on the ventral surface of the anterior process; (2) a rounded pointed triangular flange of the ~~ventero~~lateral tuberosity; (3) a laterally deflected triangular flange; and (4) the lack of a transverse ridge on the ventral surface of the pars cochlearis.

Comparisons with other fossil mysticetes (additional details in Supp. Mat.)

As a stem balaenopteroid, the holotype specimen of *Norrisanima* shares some similarities with other stem balaenopteroids and fossil mysticetes of similar age, including ‘*Balaenoptera*’ *siberi* Pilleri, 1989 (also see Pilleri 1990), ‘*Megaptera*’ *hubachi* Dathe, 1983 and *Incakujira anillodefuego* Marx and Kohno (2016). *Norrisanima* has a rostrum broadly similar to all of these taxa, although the incompleteness of the type specimen makes comparisons difficult; indeed few fossil balaenopteroid taxa (either crown or stem) preserve the entire rostral margin intact. The lateral process of the maxilla in *Norrisanima* is not a perpendicular deflection as in *Protororqualus cuvieri* Bisconti (2007b), but about 120° from the midline, more like *Incakujira*, ‘*B.*’ *siberi*, and *Plesiobalaenoptera quarantellii* Bisconti (2010a).

The overall shape of the nasal in *Norrisanima* is somewhat similar to ‘*B.*’ *siberi*, ‘*M.*’ *hubachi* (Bisconti, 2010b) and *Protororqualus cuvieri* Bisconti (2007b), but the laterally even and rectilinear nasal outlines of *Norrisanima* are unique; all other stem and crown balaenopteroids have nasals that taper posteriorly. On the dorsal surface of the nasal, *Norrisanima* possess an anterolateral flange similar, but longer, than those present in *B. edeni* (Omura et al 1981). In dorsal view, *Archaeobalaenoptera castriarquati* Bisconti (2007a) has an anterolateral corner of the nasal that exceeds the anterior level of the anteromedial corner, but there is no flange as in *Norrisanima*. Although somewhat incomplete, the remains of what appears to be a relatively thick premaxilla near the anterior termination of the nasals *Norrisanima* is similar that found in small to mid-sized *Balaenoptera* spp., such as *B. acutorostrata* and *B. edeni*, and less like the

thinner terminations in *Archaeobalaenoptera*, *Incakujira*, *Parabalaenoptera*, *Protororqualus* and ‘*M.*’ *hubachi*.

The medial surface of the supraorbital process of the frontal does not slope to the vertex as in true cetotheriids, such as *Joumocetus shimizui* Kimura & Hasegawa (2010), although it is not as sharply tabular, where the vertex is stepped above the level of the frontal, as in ‘*B.*’ *siberi*, *Incakujira*, and *Balaenoptera* spp. Generally, the ~~dimensions of the~~ vertex in *Norrisanima* ~~are~~ ~~laterally~~ wide (relative to the length of the nasals), ~~and much narrower~~ in *Archaeobalaenoptera*, *Incakujira*, *Parabalaenoptera*, *Protororqualus*, and even ‘*M.*’ *hubachi*. The dorsal junction of the maxilla and frontal that forms Demere et al. (2005)’s so-called “balaenopterid pocket” is lightly visible in *Norrisanima*, apparently to the same degree as ‘*M.*’ *hubachi*, but certainly not as strongly delineated as in *Archaeobalaenoptera*, ‘*B.*’ *siberi*, *Incakujira*, *Protororqualus* and living *Balaenoptera* and *Megaptera*. In dorsal view, the postorbital process ~~of the supraorbital~~ ~~process~~ of the frontal in *Norrisanima* is sharply angular and notably overlays the zygomatic process of the squamosal; this combination of features is clear in *Incakujira*, slightly overlapping in ‘*M.*’ *hubachi*, but notably absent in other stem balaenopteroids with complete supraorbital processes of the frontals, such as *Parabalaenoptera*.

In *Norrisanima*, the anterior margin of the supraoccipital shield is essentially at the level of preorbital process, in dorsal view, which is broadly similar to living *Megaptera* and *B. acutorostrata*, but unlike all other living *Balaenoptera* spp. The position of this margin in *Norrisanima* is anterior to most other stem balaenopteroids, where it is shifted more posteriorly, as in ‘*M.*’ *hubachi*, *Parabalaenoptera*, ‘*B.*’ *siberi*, *Balaenoptera bertae* Boessenecker (2012) and

685 *Incakujira*. Also, the shape of this margin in *Norrisanima* is broadly semi-lunar and evenly
 686 ovate, not sharply acute as in *Incakujira*, *Parabalaenoptera*, and *B. bertae*, or with the irregular
 687 lobate margin as in ‘*M.*’ *hubachi*. The lateral margin of the supraoccipital, extending to the
 688 nuchal crests, overhangs the posterior margin of the temporal wall in *Norrisanima*, as it does in
 689 most other fossil balaenopteroids, but not *Archaeobalaenoptera*. In shape and relative position to
 690 the frontal, the supraoccipital *Norrisanima* shares little with *Archaeobalaenoptera* and
 691 *Protororqualus*. No interparietal is visible in the dorsal vertex of *Norrisanima*, although it is
 692 possible that part of the parietals are exposed along the lateral margins of the vertex; it is difficult
 693 to ascertain because of poor preservation.

694

695 The length and lateral deflection of the zygomatic processes of the squamosal in *Norrisanima*
 696 resembles that living *Balaenoptera* spp., and especially *Megaptera*. Like many fossil
 697 balaenopteroids, the postglenoid process and the posterolaterally facing suprimeatal fossa are not
 698 visible in dorsal view of the basicranium of *Norrisanima*, with the proportion of the width of the
 699 paraoccipitals, relative to the bizygomatic width, is more like that in *Incakujira*,
 700 *Parabalaenoptera* and ‘*M.*’ *hubachi* than living *Balaenoptera* and *Megaptera*. The entire ventral
 701 side of the basicranium in *Norrisanima* is broadly proportioned like living *Balaenoptera* and
 702 *Megaptera*, in terms of the relative spacing of the glenoid fossae to the distance between the
 703 pterygoid sinuses, and the anteroposterior length across the temporal walls.

704

705 **Late Miocene marine mammal assemblages from California and phylogenetic divergences**
 706 *Norrisanima* was collected from late Miocene age diatomite sequences of southern California
 707 that have also yielded a variety of large marine vertebrates, including type specimens of

Pithanotaria and *Imagotaria*, and a variety of other seabird and fossil vertebrate taxa. The Tortonian age constraints of *Norrisanima* (7.6–7.3 Ma) potentially also apply to *Pithanotaria* and *Imagotaria*, which were collected from likely coeval units of the diatomite sequences from the type locality of *Norrisanima*, which collectively provide narrower stratigraphic intervals on divergence dates for clades related to these taxa. For example, *Pithanotaria* is a crown otariid according to recent analyses (Velez-Juarbe 2017), and as the oldest crown lineage, its age constrains the divergence time for this clade. Similarly, *Norrisanima*'s position outside of crown Balaenopteroidea may provide similar constraints on the divergence date for this crown clade, although its stratigraphic age is younger than less well constrained ~~than~~ late Miocene age eschrichtiids (e.g., '*B.*' *portisi*) that consistently group inside crown Balaenopteroidea (see Demere et al. 2005; Slater et al. 2007). This late Miocene divergence time also is strikingly young compared to other molecular-based inferences of phylogenetic divergence for this clade (e.g., McGowen et al. 2009).

Acknowledgements

We thank M. Dattoria, J. Conrad, V. Rossi, A. Metallo, and the Smithsonian Institution's Digitization Program Office 3D Lab for training, technical support, and access to equipment. We also thank J. Hinton and S. Sholts of the Smithsonian Institution Bio-Imaging Research Center in the Department of Anthropology at the National Museum of Natural History for assistance CT scanning the tympanoperiotic material. MSL thanks the Smithsonian Office of Fellowships and Internships—especially A. Lemon and A. Capobianco—for their assistance during his James Smithson and Secretary's Distinguished Research Postdoctoral Fellowship. NDP thanks the Basis Foundation and its Remington Kellogg Fund for support. Finally, we thank E. Coombs, E.

Noirault, A. Goswami, and R. Sabin for access to 3D digital models from the Natural History Museum London.

Author contributions

MSL, CMP, & NDP conceived and designed the experiments, performed the experiments, analyzed the data, contributed reagents/materials/analysis tools, wrote the paper, prepared figures and/or tables, and reviewed drafts of the paper.

Figure Captions:

Figure 1. Three frequently reoccurring phylogenetic hypotheses of the relationship between Balaenopteridae and Eschrichtiidae, as well as the relative placement of *N. miocaena*. Note the uncertainty regarding the placement of *N. miocaena* inside the balaenopterids, inside the clade Megaptera, and outside crown Balaenopteroidea (see text for further description of the data types and taxon sampling that support these hypotheses). Crown symbol designates crown Balaenopteroidea.

Figure 2. Holotype skull (USNM 10300) of *Norrisanima miocaena* in dorsal view. A. Dorsal view taken from 3D model created by laser scanning. B. Illustrated with a low opacity mask and interpretive line art. Cross-hatching is matrix or plaster. Dotted lines indicate broken or missing fragments. To view the 3D model of the specimen, visit the Smithsonian X 3D website at (<http://3d.si.edu>).

Figure 3. Holotype skull (USNM 10300) of *Norrisanima miocaena* in ventral view. A.

Ventral view taken from 3D model created by laser scanning. B. Illustrated with a low opacity mask and interpretive line art. Cross-hatching is matrix or plaster. Dotted lines indicate broken or missing fragments. To view the 3D model of the specimen, visit the Smithsonian X 3D website at (<http://3d.si.edu>).

Figure 4. Right tympanic bulla of the holotype (USNM 10300) of *Norrisanima miocaena*.

Image taken from 3D model created by CT scanning and illustrated with a low opacity mask and interpretive line art: A. dorsal, B. ventral, C. medial, D. lateral, E. anterior, F. posterior. Cross-hatching is matrix or plaster. To view the 3D model of the specimen, visit the Smithsonian X 3D website at (<http://3d.si.edu>).

Figure 5. Right periotic of the holotype (USNM 10300) of *Norrisanima miocaena*. Image

taken from 3D model created by CT scanning: A. dorsal, B. ventral, C. lateral, D. medial. To view the 3D model of the specimen, visit the Smithsonian X 3D website at (<http://3d.si.edu>).

Figure 6. Comparisons of the vertex and dorsal surface of the cranium of *Norrisanima*

miocaena* with some extant baleen whale species based on available 3D models. A. *Caperea

***marginata* Gray 1846 (NHMUK 1876.2.16.1), B. *Eubalaena australis* (NHMUK 1873.3.3.1), C.**

Balaenoptera edeni* Anderson 1878 (NHMUK 1920.12.31.1), D. *Megaptera novaeangliae

Borowski 1781 (NHMUK 792a), E. *Norrisanima miocaena* (USNM 10300), F. *B. physalus*

(NHMUK 1862.7.18.1), G. *B. acutorostrata* (NHMUK 1965.11.2.1), H. *B. borealis* (NHMUK

1934.5.25.1), I. *B. musculus* (NHMUK 1892.3.1.1). All NHMUK scans were downloaded from <https://doi.org/10.5519/0020467>, with the exception of the blue whale which was acquired from https://sketchfab.com/NHM_Imaging (Sabin et al 2018), and humpback whale, which was made available directly from the NHMH to the authors.

Fig. 7. Comparisons of the right periotic of *Norrisamina miocaena* with extant species within *Balaenoptera* and *Megaptera* (except for C, all specimens are the right periotic; all are shown in ventral view with the anterior oriented up). A. *Balaenoptera bonaerensis* (USNM 504953), B. *B. borealis* (USNM 504699) C. *B. physalus* (USNM 237566), D. *Norrisamina miocaena* (USNM 10300), E. *Megaptera novaeangliae* (USNM 486175). *N. miocaena* is enlarged with a scale bar at 1cm; the scale bar for other periotics is 10cm. Numbered characters are listed in Table S1: 1) Aperture of cranial nerve (CN) ducts deeply recessed in pars cochlearis (PC), 2) Aperture of CN ducts erupt medial; not deflected dorsally, 3) Dorsoventrally flat and mediolaterally elongate PC, 4) Short and robust anterior process (AP) relative to size of PC, 5) Presence of lateral crest on the ventral surface of AP, 6) Sharply pointed triangular flange, 7) Posteriorly deflected triangular flange, 8) Concave medial margin of PC, 9) Transverse ridge on ventral surface of PC, 10) Deep invagination of fenestra ovalis.

References:

- Akiba F. 1986. Taxonomy, morphology and phylogeny of the Neogene diatom zonal marker species in the middle-to-high latitudes of the North Pacific. *Deep Sea Drilling Project Initial Reports* 87:483-554.
- Anderson J. 1879. Balaenoptera. Cetacea Anatomical and zoological researches: Comprising an account of the zoological results of the two expeditions to Western Yunnan in 1868 and 1875; and a monograph of the two cetacean genera, platanista and orcella. 551-564. London: Bernard Quaritch.
- Árnason Ú, Lammers F, Kumar V, Nilsson MA. and Janke, A., 2018. Whole-genome sequencing of the blue whale and other rorquals finds signatures for introgressive gene flow. *Science Advances* 4(4), p.eaap9873. DOI: 10.1126/sciadv.aap9873.
- Barron JA, 1986. Paleooceanographic and tectonic controls on deposition of the Monterey Formation and related siliceous rocks in California. *Palaeogeography, Palaeoclimatology, Palaeoecology* 53(1), pp.27-45.
- Barron JA, and Isaacs CM. 2001. Updated chronostratigraphic framework for the California Miocene. *The Monterey Formation: from Rocks to Molecules* 10:393.
- Barron JA, Lyle M, and Koizumi I. 2001. Late Miocene and early Pliocene biosiliceous sedimentation along the California margin. *Revista Mexicana de Ciencias Geológicas* 19(3):161-169. DOI:
- Behl RJ, Ramirez PC, and Stanley RG. 2000. Field Guide to the Geology of the Neogene Santa Maria Basin: From Rift to Uplift.

- 817 Bisconti M. 2007a. A new balaenopterid whale from the Pliocene of northern Italy. *Paleontology*
818 50(5):1103-1122. 10.1111/j.1475-4983.2007.00696.x.
- 819 Bisconti M. 2007b. Taxonomic revision and phylogenetic relationships of the rorqual-like
820 mysticete from the Pliocene of Mount Pulgnasco, northern Italy (Mammalia, Cetacea,
821 Mysticeti). *Paleontographica Italica* 91:85-108. DOI: 10.1080/02724631003762922.
- 822 Bisconti M. 2010a. A new balaenopterid whale from the Late Miocene of the Stirone River,
823 northern Italy (Mammalia, Cetacea, Mysticeti). *Journal of Vertebrate Paleontology*
824 30:943-958. DOI: 10.1080/02724631003762922.
- 825 Bisconti M. 2010b. New description of "*Megaptera*" *hubachi* Dathe, 1983, based on the holotype
826 skeleton held in the Museum für Naturkunde, Berlin. 2010. *Quaderni del Museo di Storia*
827 *Naturale di Livorno* 23:37-68. DOI: 10.4457/musmed.2010.23.37.
- 828 Boessenecker RW. 2012. A new marine vertebrate assemblage from the Late Neogene Purisima
829 Formation in Central California, part II: Pinnipeds and Cetaceans. *Geodiversitas*,
830 35(4):815-940. DOI: 10.5252/g2013n4a5
- 831 Boessenecker RW, and Fordyce RE. 2015. Anatomy, feeding ecology, and ontogeny of a
832 transitional baleen whale: a new genus and species of Eomysticetidae (Mammalia:
833 Cetacea) from the Oligocene of New Zealand. *PeerJ* 3: e1129. DOI: 10.7717/peerj.1129.
- 834 Boessenecker RW, and Fordyce RE. 2017. A new eomysticetid from the Oligocene Kokoamu
835 Greensand of New Zealand and a review of the Eomysticetidae (Mammalia, Cetacea).
836 *Journal of Systematic Palaeontology*, 15(6):429-469. DOI:
837 10.1080/14772019.2016.1191045.

- 838 Borowski GH. 1781. Gemeinnützige Naturgeschichte des Thierreichs: darinn die
- 839 merkwürdigsten und nützlichsten Thiere in systematischer Ordnung beschrieben und alle
- 840 Geschlechter in Abbildungen nach der Natur vorgestellt warden. Berlin 2(1).
- 841 Bosselaers M, and Post K, 2010. A new fossil rorqual (Mammalia, Cetacea, Balaenopteridae)
- 842 from the Early Pliocene of the North Sea, with a review of the rorqual species described
- 843 by Owen and Van Beneden. *Geodiversitas* 32(2):331-363. DOI: 10.5252/g2010n2a6.
- 844 Brisson MJ. 1762. *Regnum Animale in classes IX distributum, sive synopsis methodica, Ed. 2.*
- 845 Burmeister H. 1867. Preliminary description of a new species of Finner Whale. *Proceedings of*
- 846 *the Zoological Society of London* 1867:707-713.
- 847 Cantino PD, & De Queiroz K. 2014. PhyloCode: a phylogenetic code of biological
- 848 nomenclature. (Version 4c). Ohio University. Available at
- 849 <http://www.ohiou.edu/phylocode>
- 850 Chang AS, and Grimm KA. 1999. Speckled beds: distinctive gravity-flow deposits in finely
- 851 laminated diatomaceous sediments, Miocene Monterey Formation, California. *Journal of*
- 852 *Sedimentary Research* 69. DOI: 10.2110/jsr.69.122.
- 853 Cignoni P, Callieri M, Corsini M, Dellepiane M, Ganovelli F, and Ranzuglia G. 2008. Meshlab:
- 854 an open-source mesh processing tool. Eurographics Italian Chapter Conference. 129-136.
- 855 DOI: 10.2312/LocalChapterEvents/ItalChap/ItalianChapConf2008/129-136

856 Deméré TA, Berta A, and McGowen MR. 2005. The taxonomic and evolutionary history of
857 fossil and modern balaenopteroid mysticetes. *Journal of Mammalian Evolution* 12:99-
858 143. DOI:10.1007/s10914-005-6944-3.

859 Deméré TA, McGowen MR, Berta A, and Gatesy J. 2008. Morphological and molecular
860 evidence for a stepwise evolutionary transition from teeth to baleen in mysticete whales.
861 *Systematic Biology*, 57(1): 15-37. DOI: 10.1080/10635150701884632

862 Desmoulins A. 1822. Baleine. Balaena. Mam. In: Dictionnaire Classique d'Histoire naturelle. 2:
863 155-165. Paris: Rey et Gravier.

864 Dibblee TW Jr. 1950. Geology of southwestern Santa Barbara County, California. *California*
865 *Division of Mines Bulletin* 105: 1-95.

866 Ekdale EG, Berta A, and Deméré TA. 2011. The comparative osteology of the petrotympanic
867 complex (ear region) of extant baleen whales (Cetacea: Mysticeti). *PLoS ONE* 6:e21311.
868 DOI: 10.1371/journal.pone.0021311.

869 Fordyce RE, & de Muizon C. 2001. Evolutionary history of cetaceans: a review. *Secondary*
870 *adaptation of tetrapods to life in water*, 169-233.

871 Gatesy J, Geisler JH, Chang J, Buell C, Berta A, Meredith RW, Springer MS, and McGowen
872 MR. 2013. A phylogenetic blueprint for a modern whale. *Molecular Phylogenetics and*
873 *Evolution* 66:479-506. DOI: 10.1016/j.ympev.2012.10.012.

874 Geisler JH, Boessenecker RW, Brown M, and Beatty BL. 2017. The origin of filter feeding in
875 whales. *Current Biology* 27(13):2036-2042. DOI: 10.1016/j.cub.2017.06.003

- 876 Geisler JH, McGowen MR, Yang G, Gatesy J. 2011. A supermatrix analysis of genomic,
877 morphological, and paleontological data from crown Cetacea. *BMC Evolutionary Biology*
878 11:112. DOI:10.1186/1471-2148-11-112

- 879 Gray JE. 1846. On the cetaceous animals. The zoology of the voyage of H. M. S. Erebus and
880 Terror, under the command of Capt. Sir J. C. Ross, R. N., F. R. S., during the years 1839
881 to 1843 1 & 2:1-53.

- 882 Gray JE. 1864. On the Cetacea which have been observed in the seas surrounding the British
883 Islands. *Proceedings of the Scientific Meetings of the Zoological Society of London*
884 1864:195-248.

- 885 Gray JE. 1868. Synopsis of the species of whales and dolphins in the Collection of the British
886 Museum 1-10.

- 887 Joyce WG, Parham JF, & Gauthier JA. 2004. Developing a protocol for the conversion of rank-
888 based taxon names to phylogenetically defined clade names, as exemplified by turtles.
889 *Journal of Paleontology* 78(5): 989-1013.

- 890 Kellogg R. 1922. Description of the skull of *Megaptera miocaena*, a fossil humpack whale from
891 the Miocene diatomaceous earth of Lompoc, California. *Proceedings of the U S National*
892 *Museum* 61:18P.

- 893 Kellogg R. 1925. New pinnipeds from the Miocene diatomaceous earth near Lompoc, California.
894 *Contributions to Palaeontology from the Carnegie Institution of Washington* 348:71-95.

- 895 Kellogg R. 1965. A new whalebone whale from the Miocene Calvert Formation. *Bulletin of the*
896 *United States National Museum* 247(1):1-45.
- 897 Kimura T, & Hasegawa Y. 2010. A new baleen whale (Mysticeti: Cetotheriidae) from the
898 earliest late Miocene of Japan and a reconsideration of the phylogeny of cetotheres.
899 *Journal of Vertebrate Paleontology* 30(2): 577-591.
- 900 Kleinpell RM. 1938. Miocene stratigraphy of California. American Association of Petroleum
901 Geologists. Tulsa, Oklahoma. 450 p.
- 902 Lacépède B. 1804. Histoire naturelle des cétacés. Paris: P. Didot l'ainé et Firmin Didot.
- 903 Linnaeus C. 1758. Systema Naturae per Regna Tria Naturae, Secundum Classes, Ordines,
904 Genera, Species, cum Characteribus, Differentiis, Synonymis, Locis. Editio Decima 1: 1-
905 824.
- 906 Marx FG. 2011. The more the merrier? A large cladistic analysis of mysticetes, and comments
907 on the transition from teeth to baleen. *Journal of Mammal Evolution* 18: 77-100 DOI
908 10.1007/s10914-010-9148-4.
- 909 Marx FG, and Fordyce RE. 2015. Baleen boom and bust: a synthesis of mysticete phylogeny,
910 diversity and disparity. *Royal Society Open Science* 2(4): 140434. DOI:
911 10.1098/rsos.140434.
- 912 Marx FG, and Kohno N. 2016. A new Miocene baleen whale from the Peruvian desert. *Royal*
913 *Society Open Science* 3:160542. DOI: 10.1098/rsos.160542.

- 914 McGowen MR, Spaulding M. and Gatesy J. 2009. Divergence date estimation and a
915 comprehensive molecular tree of extant cetaceans. *Molecular Phylogenetics and*
916 *Evolution*, 53(3): 891-906. DOI: 10.1016/j.ympev.2009.08.018.
- 917 Mead JG, and Fordyce RE. 2009. The therian skull: a lexicon with emphasis on the odontocetes.
918 *Smithsonian Contributions to Zoology*: 1-248. DOI: 10.5479/si.00810282.627.
- 919 Mitchell ED. 1968. The Mio-Pliocene pinniped Imagotaria. *Journal of the Fisheries Research*
920 *Board of Canada* 25(9):1843-1900.
- 921 Oishi M, & Hasegawa Y. 1994. A list of fossil cetaceans in Japan. *Island Arc* 3(4): 493-505.
- 922 Omura H, Kasuya T, Kato H, Wada S. 1981. Osteological study of the Bryde's whale from the
923 central south Pacific and eastern Indian Ocean. *Scientific Report of the Whales Research*
924 *Institute*, 33: 1-26
- 925 Parham JF, Donoghue PC, Bell CJ, Calway TD, Head JJ, Holroyd PA, Inoue JG, Irmis RB,
926 Joyce WG, Ksepka DT, Patané JS, et al. 2012. Best practices for justifying fossil
927 calibrations. *Systematic Biology*, 61(2):346-359. DOI: 10.1093/sysbio/syr107.
- 928 Pilleri G. 1989. Balaenoptera siberi, ein neuer spätmiozäner Bartenwal aus der Pisco-Formation
929 Perus. *Beiträge zur Paläontologie der Cetaceen Perus Hirnanatomisches Institut*
930 *Ostermündingen, Bern*:63-84.
- 931 Pilleri G. 1990. Paratypus von Balaenoptera siberi (Cetacea: Mysticeti) aus der Pisco Formation
932 Perus. *Beiträge zur paläontologie der cetaceen und pinnipedier der Pisco Formation*

- 933 *Perus II Waldau-Berne, Switzerland: Hirnanatomisches Istitut der Universitat Bern*
- 934 *Ostermundigen (Schweiz) p:205-215.*
- 935 Pyenson ND, Vélez-Juarbe J, Gutstein CS, Little H, Vigil D, & O'Dea A. 2015. Isthminia
- 936 panamensis, a new fossil inioid (Mammalia, Cetacea) from the Chagres Formation of
- 937 Panama and the evolution of 'river dolphins' in the Americas. *PeerJ*, 3, e1227.
- 938 doi:10.7717/peerj.1227.
- 939 Pyenson ND, and Sponberg SN. 2011. *Journal of Mammal Evolution* 18: 269. DOI:
- 940 10.1007/s10914-011-9170-1.
- 941 Repenning CA, and Tedford RH. 1977. Otarioid seals of the Neogene. *United States Geological*
- 942 *Survey Professional Paper* 992:1-93.
- 943 Rice D. 1998. Marine mammals of the world; systematics and distribution. Special Publication 4.
- 944 Society of Marine Mammalogy. 1-231.
- 945 Sabin R, Burton K, Cooper N, Goswami A. 2018. Dataset: 3D Cetacean Scanning. Natural
- 946 History Museum Data Portal (data.nhm.ac.uk). DOI: <https://doi.org/10.5519/0020467>
- 947 Sasaki, T., Masato N, Wada S, Yamada TK, Cao Y, Hasegawa M, Okada N. 2006. *Balaenoptera*
- 948 *omurai* is a newly discovered baleen whale that represents an ancient evolutionary
- 949 lineage. *Molecular Phylogenetics and Evolution* 41(1): 40-52. DOI:
- 950 10.1016/j.ympev.2006.03.032

- 951 Slater GJ, Goldbogen JA, and Pyenson ND. 2017. Independent evolution of baleen whale
952 gigantism linked to Plio-Pleistocene ocean dynamics. *Proceedings of the Royal Society*
953 *B: Biological Sciences* 284. DOI: 10.1098/rspb.2017.0546

- 954 Uhen MD. 2008. New protocetid whales from Alabama and Mississippi, and a new cetacean
955 clade, Pelagiceti. *Journal of Vertebrate Paleontology* 28(3):589-593

- 956 Zeigler CV, Chan GL, and Barnes LG. 1997. A new Late Miocene balaenopterid whale (Cetacea
957 Mysticeti), *Parabalaenoptera baulinensis*, (new genus and species) from the Santa Cruz
958 Mudstone, Point Reyes Peninsula, California. *Proceedings of the California Academy of*
959 *Sciences* 50:115-138.
- 960

Table 1 (on next page)

Ten characters of the periotic that broadly distinguish *Balaenoptera* and *Megaptera*, and how *Norrisanima* compares to these genera (Y/N).

Column abbreviations: B = *Balaenoptera*; M = *Megaptera*, N = *Norrisanima*. Character abbreviations: PC = pars cochlearis; CN = cranial nerves; AP = anterior process. View abbreviations: M = medial, D = dorsal, V = ventral.

Tables:

Table 1. Ten characters of the periotic that broadly distinguish *Balaenoptera* and *Megaptera*, and how *Norrisanima* compares to these genera (Y/N). Column abbreviations: B = *Balaenoptera*; M = *Megaptera*, N = *Norrisanima*. Character abbreviations: PC = pars cochlearis; CN = cranial nerves; AP = anterior process. View abbreviations: M = medial, D = dorsal, V = ventral.

#	Character	B	M	N	View
1	Aperture of CN ducts deeply recessed in PC	N	Y	Y	M, D
2	Aperture of CN ducts erupt medial; not deflected dorsally	N	Y	Y	M, D
3	Dorsoventrally flat and mediolaterally elongate PC	N	Y	Y	V
4	Short and robust AP relative to size of PC	N	Y	Y	V, D
5	Presence of lateral crest on the ventral surface of AP	N	Y	N	V
6	Sharply pointed triangular flange	N	Y	N	V, D
7	Posteriorly deflecting triangular flange	N	Y	N	V, D
8	Concave medial margin of PC	N	Y	Y	V, D
9	Transverse ridge on ventral surface of PC	N	Y	N	V
10	Deep invagination of fenestra ovalis	N	Y	Y	V

Figure 1

Three frequently reoccurring phylogenetic hypotheses of the relationship between Balaenopteridae and Eschrichtiidae, as well as the relative placement of *N. miocaena*

Note the uncertainty regarding the placement of *N. miocaena* inside the balaenopterids, inside the clade Megaptera, and outside crown Balaenopteroidea (see text for further description of the data types and taxon sampling that support these hypotheses). Crown symbol designates crown Balaenopteroidea.

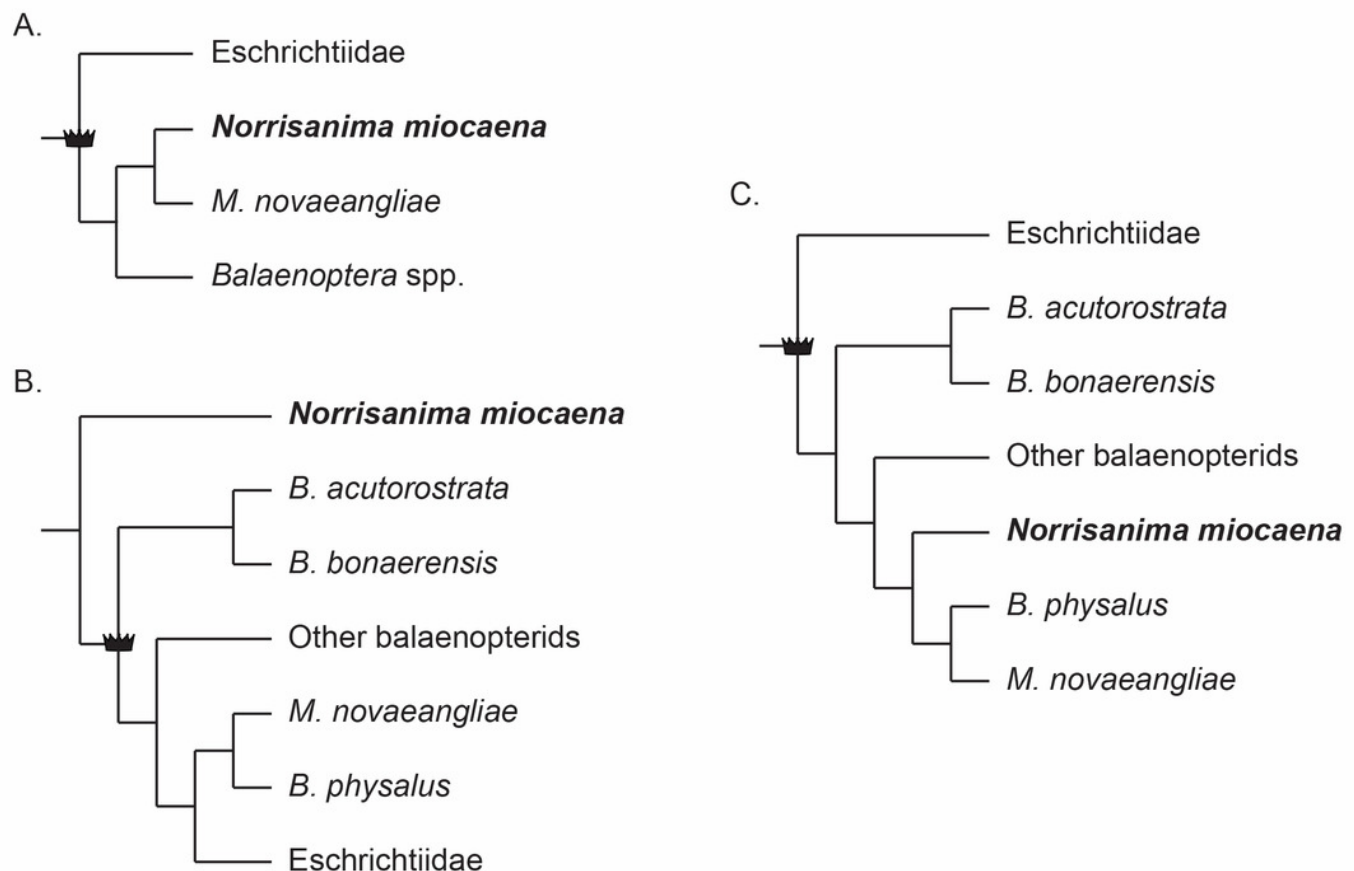
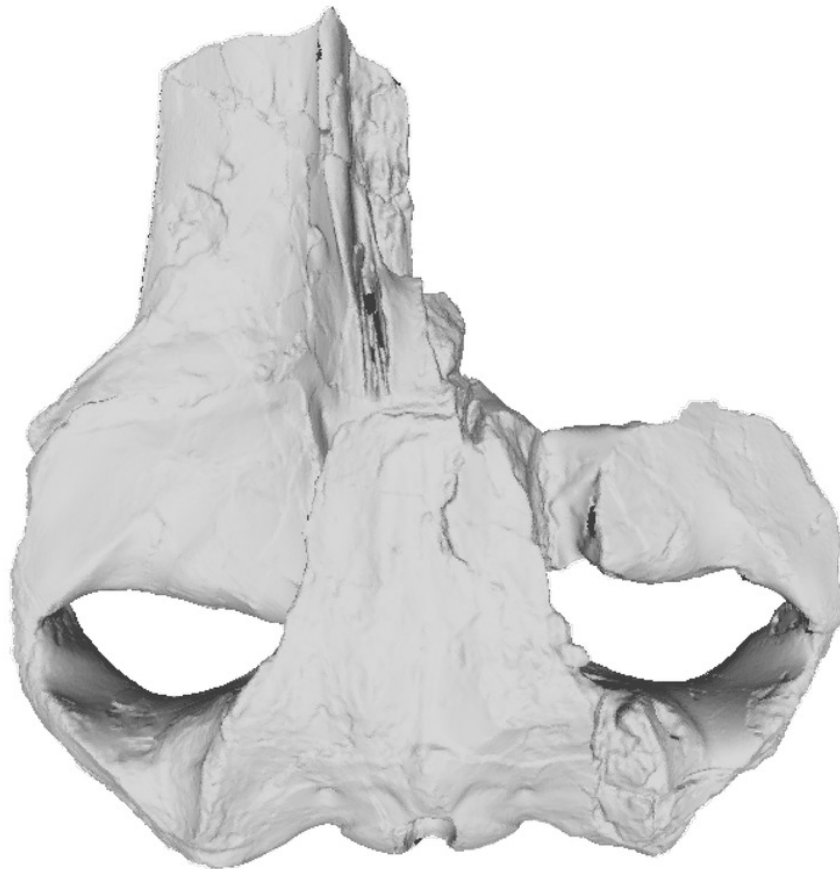


Figure 2

Holotype skull (USNM 10300) of *Norrisanima miocaena* in dorsal view

Dorsal view taken from 3D model created by laser scanning. B. Illustrated with a low opacity mask and interpretive line art. Cross-hatching is matrix or plaster. Dotted lines indicate broken or missing fragments. To view the 3D model of the specimen, visit the Smithsonian X 3D website at (<http://3d.si.edu>).

A.



B.

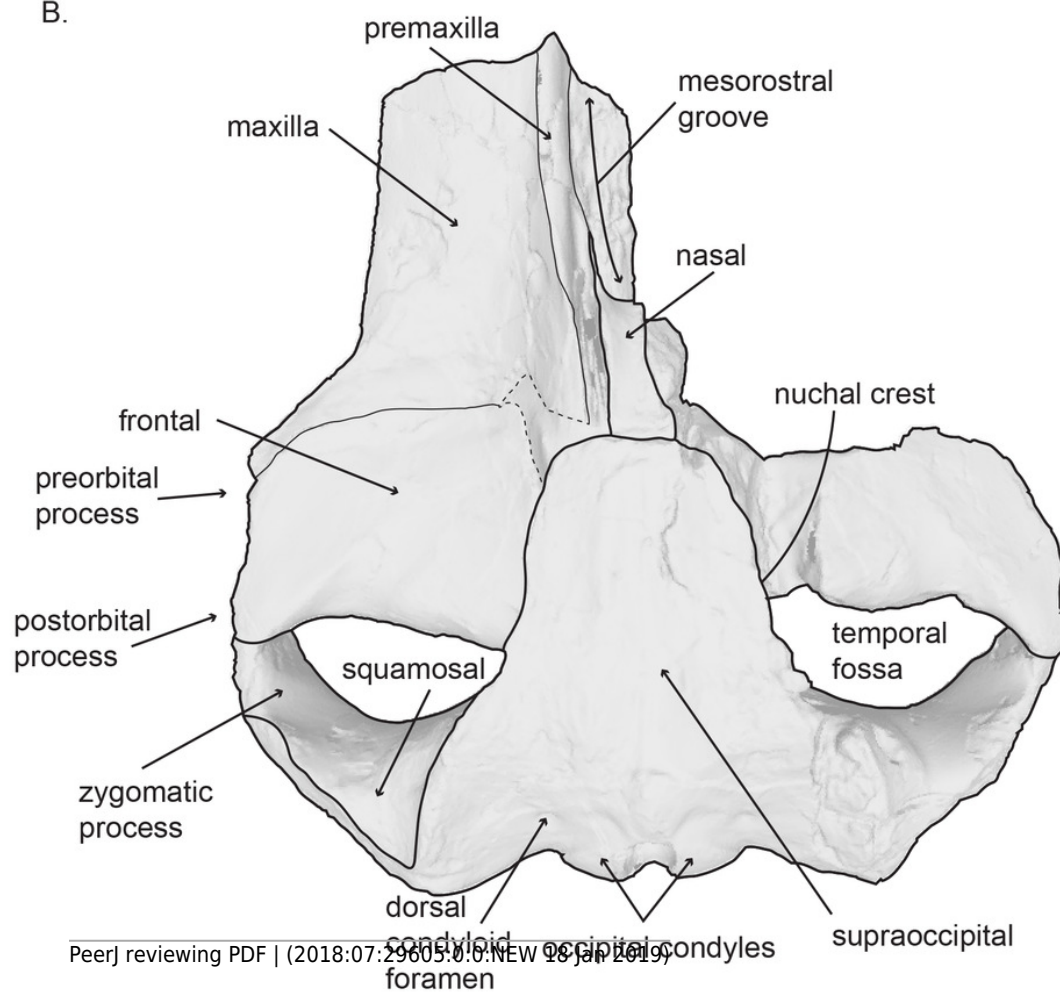


Figure 3

Figure 3. Holotype skull (USNM 10300) of *Norrisanima miocaena* in ventral view.

Ventral view taken from 3D model created by laser scanning. B. Illustrated with a low opacity mask and interpretive line art. Cross-hatching is matrix or plaster. Dotted lines indicate broken or missing fragments. To view the 3D model of the specimen, visit the Smithsonian X 3D website at (<http://3d.si.edu>).

A.



B.

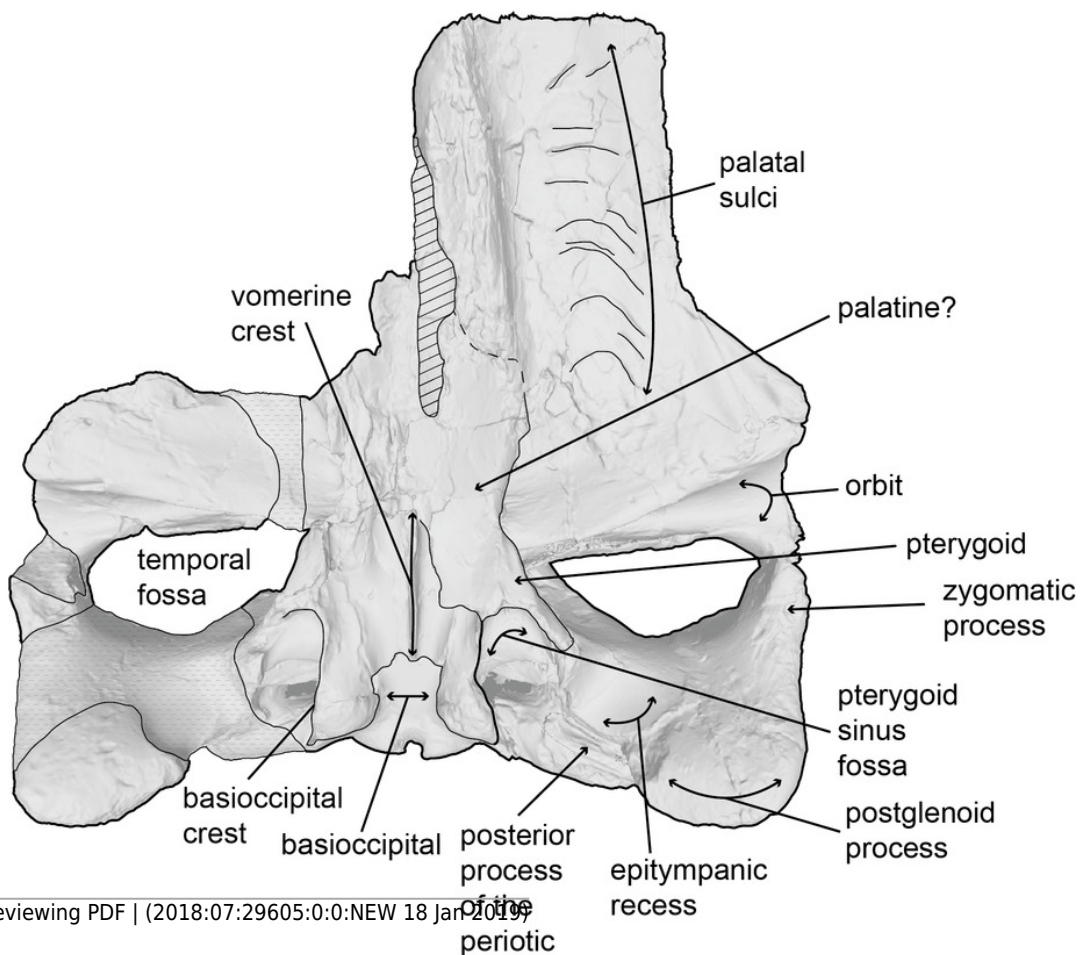


Figure 4

Right tympanic bulla of the holotype (USNM 10300) of *Norrisanima miocaena*

Image taken from 3D model created by CT scanning and illustrated with a low opacity mask and interpretive line art: A. dorsal, B. ventral, C. medial, D. lateral, E. anterior, F. posterior.

Cross-hatching is matrix or plaster. To view the 3D model of the specimen, visit the Smithsonian X 3D website at (<http://3d.si.edu>).

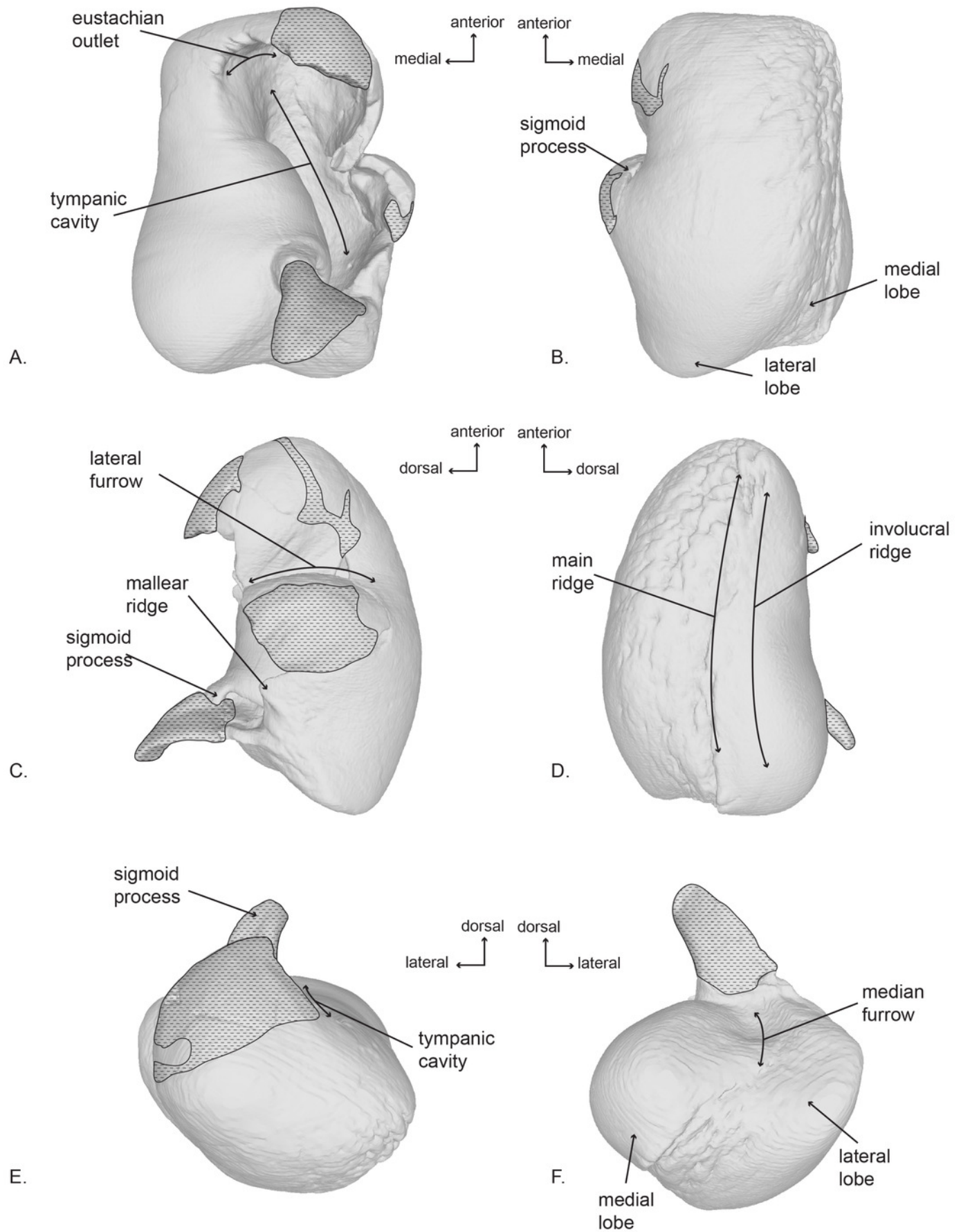


Figure 5

Right periotic of the holotype (USNM 10300) of *Norrisanima miocaena*.

Image taken from 3D model created by CT scanning: A. dorsal, B. ventral, C. lateral, D. medial. To view the 3D model of the specimen, visit the Smithsonian X 3D website at (<http://3d.si.edu>).

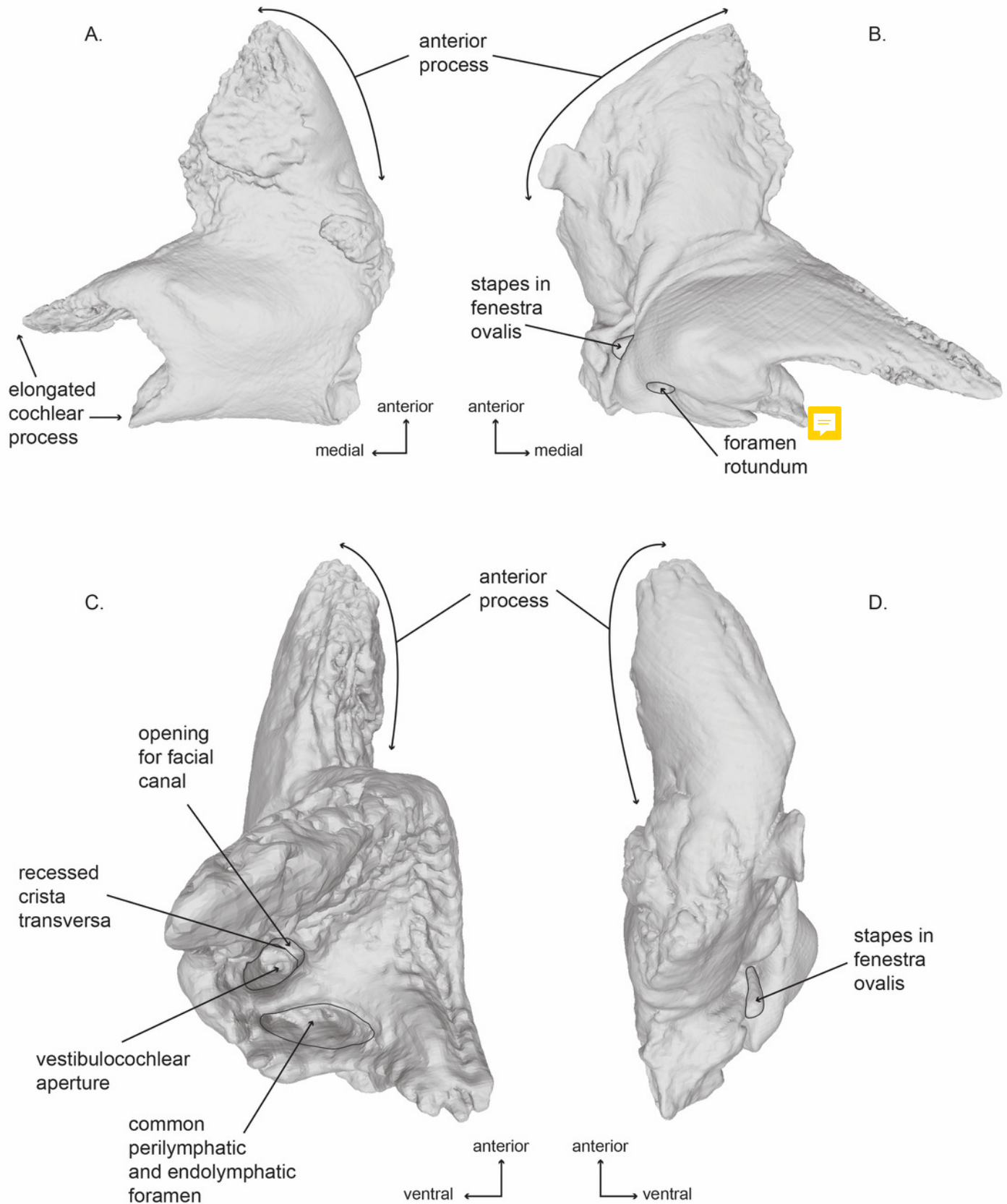


Figure 6

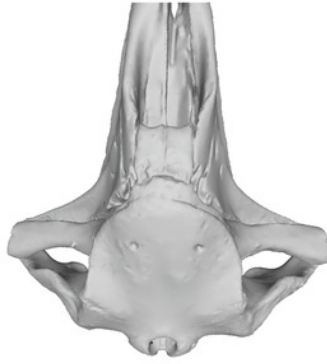
Comparisons of the vertex and dorsal surface of the cranium of *Norrisamina miocaena* with some extant baleen whale species based on available 3D models.

A. *Caperea marginata* Gray 1846 (NHMUK 1876.2.16.1), B. *Eubalaena australis* (NHMUK 1873.3.3.1), C. *Balaenoptera edeni* Anderson 1878 (NHMUK 1920.12.31.1), D. *Megaptera novaeangliae* Borowski 1781 (NHMUK 792a), E. *Norrisanima miocaena* (USNM 10300), F. *B. physalus* (NHMUK 1862.7.18.1), G. *B. acutorostrata* (NHMUK 1965.11.2.1), H. *B. borealis* (NHMUK 1934.5.25.1), I. *B. musculus* (NHMUK 1892.3.1.1). All NHMUK scans were downloaded from <https://doi.org/10.5519/0020467> , with the exception of the blue whale which was acquired from https://sketchfab.com/NHM_Imaging (Sabin et al 2018).

A. *Caperea marginata*



B. *Eubalaena australis*



C. *Balaenoptera edeni*



D. *Megaptera novaeangliae*



E. *Norrisania miocaena*



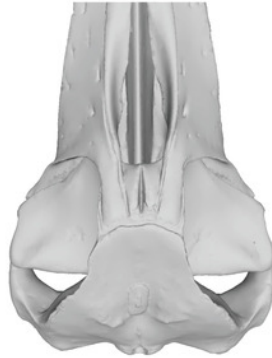
F. *Balaenoptera physalus*



G. *Balaenoptera acutorostrata*



H. *Balaenoptera borealis*



I. *Balaenoptera musculus*

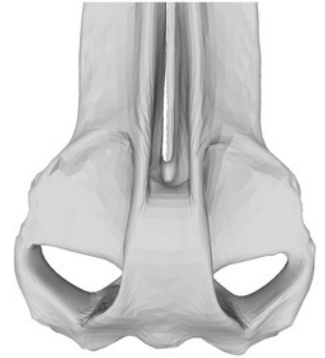


Figure 7

Comparisons of the right periotic of *Norrisamina miocaena* with extant species within *Balaenoptera* and *Megaptera* (except for C, all specimens are the right periotic; all are shown in ventral view with the anterior oriented up).

A. *Balaenoptera bonaerensis* (USNM504953), B. *B. borealis* (USNM504699) C. *B. physalus* (USNM 237566), D. *Norrisanima miocaena* (USNM 10300), E. *Megaptera novaeangliae* (USNM 486175). *N. miocaena* is enlarged with a scale bar at 1cm; the scale bar for other periotics is 10cm. Numbered characters are listed in Table S1: 1) Aperture of cranial nerve (CN) ducts deeply recessed in pars cochlearis (PC), 2) Aperture of CN ducts erupt medial; not deflected dorsally, 3) Dorsoventrally flat and mediolaterally elongate PC, 4) Short and robust anterior process (AP) relative to size of PC, 5) Presence of lateral crest on the ventral surface of AP, 6) Sharply pointed triangular flange, 7) Posteriorly deflected triangular flange, 8) Concave medial margin of PC, 9) Transverse ridge on ventral surface of PC, 10) Deep invagination of fenestra ovalis.

